UNCLASSIFIED

AD NUMBER
AD890035
LIMITATION CHANGES
TO: **Approved for public release; distribution is unlimited.**
FROM: **Distribution authorized to U.S. Gov't. agencies only; Test and Evaluation; AUG 1971. Other requests shall be referred to Air Force Armament Laboratory, Attn: DLRD, Eglin AFB, FL 32542.**
AUTHORITY
afal ltr, 24 jun 1974

THIS PAGE IS UNCLASSIFIED

AD 890035

AD No.
DDC FILE COPY

AFATL-TR-71-95

MECHANICS OF IMPACT AND CRACK PROPAGATION

PHASE I: DEVELOPMENT OF AN ANALYTICAL FRACTURE MODEL OF PROJECTILE PENETRATION

INSTITUTE OF FRACTURE AND SOLID MECHANICS
LEHIGH UNIVERSITY

TECHNICAL REPORT AFATL-TR-71-95

AUGUST 1971

DDC
RECEIVED
27 1971

TEST + EVALUATION

Distribution limited to U. S. Government agencies only: [redacted], distribution limitation applied August 1971. Other requests for this document must be referred to the Air Force Armament Laboratory (DLRD), Eglin Air Force Base, Florida 32542.

AIR FORCE ARMAMENT LABORATORY
AIR FORCE SYSTEMS COMMAND • UNITED STATES AIR FORCE
EGLIN AIR FORCE BASE, FLORIDA

114

ACCESSION for
CFSTI WHITE SECTION
DDC BUFF SECTION
UNANNOUNCED
JUSTIFICATION.....
.....
BY
DISTRIBUTION/AVAILABILITY CODES
DIST. AVAIL. and/or SPECIAL
B

Mechanics Of Impact
And
Crack Propagation

Phase I: Development Of An Analytical Fracture Model Of Projectile Penetration

G.C. Sih

G.T. Embley

TEST + EVALUATION

Distribution limited to U. S. Government agencies only; [redacted] distribution limitation applied August 1971. Other requests for this document must be referred to the Air Force Armament Laboratory (DLRD), Eglin Air Force Base, Florida 32542.

FOREWORD

This is an annual report prepared by Drs. G. C. Sih and G. T. Embley of the Institute of Fracture and Solid Mechanics, Lehigh University, Bethlehem, Pennsylvania, under Air Force Contract F08635-70-C-0120 for the period July 1970 to June 1971. The principal investigator for this project is Dr. G. C. Sih, Director of the Institute of Fracture and Solid Mechanics, and the work was administered by the Air Force Armament Laboratory, Eglin Air Force Base, Florida, under the direction of Lt. Charles L. Tyler and Mr. Leo L. Wilson.

This technical report has been reviewed and is approved.

CHARLES K. ARPKE, Lt Colonel, USAF
Chief, Weapons Effects Division

ABSTRACT

This report is concerned with the application of fracture mechanics theory to the problem of projectile penetration and the situation where an excessive amount of energy is available to damage the target material in the form of fracture followed by crack propagation. The conditions under which this phenomenom takes place depend on several parameters such as the speed and shape of the projectile and the geometry and material of the target. These conditions have been simulated in the laboratory. The present investigation deals only with the development of an analytical fracture model of the projectile penetration problem using the theory of continuum mechanics.

The amount of energy required to produce a crack of certain size in a pre-stretched plate within a very short period of time is estimated by solving a system of dual integral equations. Computer programs are being developed. In addition, the energy supplied to maintain a running crack at a certain speed is obtained with results illustrated by graphs. The effects of plasticity and rate sensitivity of the material are also discussed in this report.

T+E

Distribution limited to U.S. Government agencies only; [redacted]; distribution limitation applied August 1971. Other requests for this document must be referred to the Air Force Armament Laboratory (DLRD), Eglin Air Force Base, Florida 32542.

(The reverse of this page is blank)

TABLE OF CONTENTS

Section		Page
I.	INTRODUCTION	1
II.	DYNAMIC CRACK DRIVING FORCE	5
	2.1 General Dynamic Case for Arbitrary Crack Motion	5
	2.2 Steady State and Static Case	9
	2.3 Broberg's Problem	10
	2.4 Plastic Energy Dissipation	12
III.	SUDDEN APPEARANCE OF A CRACK	16
	3.1 Formulation of the Problem	19
	3.2 Dual Integral Equations	21
	3.3 Time Dependent Stress Field	29
IV.	PLASTICITY MODELS OF STEADY STATE CRACK EXTENSION	41
	4.1 The Dugdale Model	42
	4.2 Steady State Crack Propagation Problems	44
	4.3 Semi-Infinite Crack	46
	4.4 Constant Length Crack	55
V.	PLASTIC FLOW AROUND AN EXPANDING CRACK	65
	5.1 Crack Expanding Elastically	65
	5.2 Plastic Yielding Around the Crack	67
	5.3 Finiteness Condition	73
	5.4 Energy Release Rate	74
VI.	RESULTS	86

Appendix

Page

I. ELASTIC PROBLEMS OF UNIFORM CRACK EXTENSION..... 92

II. NUMERICAL PROCEDURE..... 95

REFERENCES.....100

LIST OF FIGURES

Figure	Title	Page
1	Arbitrary Contour Around a Moving Crack Tip	6
2	Incremental Motion of Crack Tip	8
3	Change in Displacement of Crack Surface and Elastic-Plastic Interface over Increment of Time Δt	13
4	Geometry and Load Configuration for Equivalent Elastic Problem	13
5	Crack Geometry and Stress Components	18
6	Path of Integration in w-plane	33
7	Wave Fronts Emanating from Crack Tips	36
8	Solution to the Fredholm Integral Equation	39
9	Dynamic Stress-Intensity Factor	40
10	Line Crack with Dugdale Plastic Zone	43
11	Equivalent Elastic Problem for Line Crack with Dugdale Plastic Zone	43
12	Semi-Infinite Crack Loaded with Concentrated Forces	47
13	Semi-Infinite Crack with Dugdale Plastic Zone	47
14	Equivalent Elastic Problem for Semi-Infinite Crack	47
15	Finiteness Condition for Semi-Infinite Crack	52
16	Ratio of Plastic to Elastic Energy Release Rate as a Function of Normalized Load for Semi-Infinite Crack	54
17	Constant Length Crack with Dugdale Plastic Zone Propagating with Velocity v	56
18	Constant Length Crack Propagating with Velocity v and Loaded by Concentrated Forces	58

LIST OF FIGURES (CONCLUDED)

Figure	Title	Page
19	Constant Length Crack Propagating with Velocity v and Loaded Uniformly over Portion of Crack Surface	58
20	Energy Release Rate Versus Crack Speed for Fixed Length and Semi-Infinite Dynamic Crack Models	63
21	Ratio of Plastic to Elastic Energy Release Rate as a Function of Normalized Load for Fixed Length Crack	64
22	Finiteness Condition for Uniformly Expanding Crack. Plot of Ratio of Applied to Yield Stress Versus Relative Plastic Zone Length for Various Velocities of the Tip of the Plastic Strip	75
23	Finiteness Condition for Uniformly Expanding Crack. Plot of Ratio of Applied to Yield Stress versus Relative Plastic Zone Length for Various Crack Tip Velocities	76
24	Finiteness Condition for Uniformly Expanding Crack. Plot of Normalized Velocity of Plastic Zone Tip versus Ratio of Applied to Yield Stress for Various Crack Tip Velocities	77
25	Plot of Normalized Crack Opening Displacement versus Relative Plastic Zone Length for Various Crack Tip Velocities. Valid for Constant Length Crack and Uniformly Expanding Model	78
26	Normalized Energy Release Rate for Uniformly Expanding Crack Model	82
27	Relative Difference in Energy Release Rate for Expanding Crack Model Due to Difference in Method of Calculation Plotted as a Function of Crack Velocity	84
28	Relative Difference in Energy Release Rate for Expanding Crack Model Due to Method of Calculation Plotted as a Function of P/Y	85

SECTION I

INTRODUCTION

One class of problems that has received little attention relative to its potential practical importance is that of the dynamic fracture of structures due to impact loadings. This is mainly because of the extreme complexities of the problems which involve, in addition to the inertia of the structural system, such effects as plastic deformation, rate dependent material property, non-linear behavior, etc. Lacking in particular is an understanding of the failure of structural members damaged by projectile penetration.

From a thermodynamic viewpoint, the energy input to a target material is divided into elastic strain energy, plastic energy dissipated in the form of heat, kinetic energy, and the energy carried by the projectile leaving the target material. However, if the input work exceeds the dissipation, then the unbalanced portion of the energy will be absorbed in creating new surfaces starting at the edge of a stress raiser of the damaged target. This portion of the total energy is referred to in fracture mechanics as the "surface energy" which is also associated with quantities commonly known as the energy release rate or crack driving force G and, indirectly, the stress-intensity factor k [1,2]. The relationship between G and k has been recently established by Sih [3] for all the three fundamental modes of dynamic

fracture. Hence, a knowledge of G or k will provide the basis for a more efficient assessment of how cracks, once initiated, might be stopped, and provide the first step toward the possibility of defining a dynamic fracture toughness value of a material which, in essence, determines the criterion for arresting running cracks.

The overall problem of projectile penetration is considerably more complicated since it involves not only an estimate of G or k but the proportions and transfer rates among all the energies described earlier throughout the impact process. Aside from the fracture energy, it is also important to know the portion of the total energy that is dissipated through transformation of the target material which undergoes a transition from the fluid to solid state during and after impact. A study of the material flow process will involve the assumption of an appropriate constitutive equation and a numerical scheme which necessitates large scale computations. The final configuration of the damaged target, such as hole diameter and the extent or speed of petalling cracks, depends on the distribution of the remaining input energy.

The material flow process concerned with the formation of holes in plates or the perforation of impacted plates has been studied by Taylor [4], Chen [5], and others [6,7]. This report deals mainly with crack formation under impact and the conditions under which the cracks or flaws might

trigger catastrophic failure of the target material. To this end, the first year effort has been devoted to assess the amount of energy dissipated by the sudden appearance of a crack in a prestretched target material, a crack running at a constant speed, and the effect of plastic deformation ahead of a moving crack. Other considerations, such as crack acceleration and rate sensivity of the material, will be treated in the future.

A general expression for the dynamic energy release rate of a crack undergoing arbitrary motion is developed in Section II. This is essentially the work done for opening a line segment ahead of the crack. For constant crack velocity, the expression reduces to that of the path independent integral derived in [3].

The problem of transient loading on a crack is considered in Section III. Use is made of integral transforms coupled with the technique of Cagniard [8] used for solving geophysics problems. There are several ways that this model may be of use. For example, perforation of a stressed plate (or pressure vessel) by spall debris could result in what may be approximated as the sudden appearance of a crack and subsequently lead to catastrophic failure. In an unstressed plate the projectile itself could create and, over a short period of time, load a crack. Such a crack can be seen in Figure 78 of Reference [9]. The results in terms of dynamic stress-intensity factors are plotted as a function of time.

In Section IV, several models of propagating cracks are considered. Through use of a simple model, in which the plastic yielding is assumed to occur in a narrow region ahead of the running crack, the amount of energy dissipated in the various running crack models is calculated. This information is essential in estimating the fracture energy of the projectile penetration process.

Thus, the overall objective of understanding the projectile penetration problem will be accomplished by first solving a number of idealized problems where the various effects can be treated separately. Evaluation of the problem as a whole requires a coordinated effort of research in several areas which are still being investigated.

SECTION II

DYNAMIC CRACK DRIVING FORCE

An expression is derived here for the energy release rate associated with a moving crack tip. This derivation is, in principle, the same as that given by Atkinson and Eshelby [10] in consideration of the Broberg model [11] which deals with the case of a constant velocity crack running at both ends. This provides the basis for computing the amount of energy released by a running crack in the target material after impact.

The general expression derived in Section 2.1 does not depend on behavior of crack velocity with respect to time. Subsequent reduction is made for uniform crack extension both for a steady state and non-steady state of stress ahead of the crack. The general result for both of these cases of uniform crack extension may be written in terms of a contour integral which Sih [3] has shown to be path independent. The energy calculation for the problem of a uniformly expanding crack with a Dugdale-type plastic zone is treated separately as the general expression cannot be readily applied.

2.1 GENERAL DYNAMIC CASE FOR ARBITRARY CRACK MOTION

An energy balance must be written for a contour C enclosing the tip of a crack moving with a constant velocity v as shown in Figure 1.

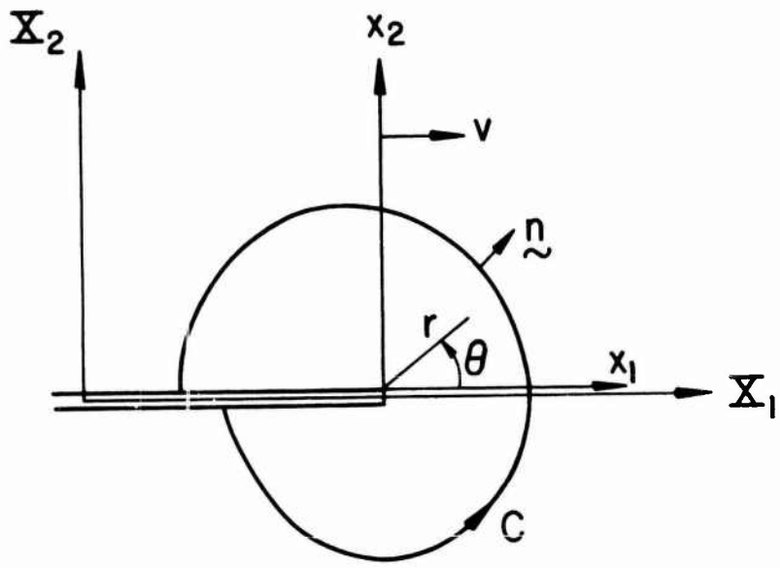

Figure 1. Arbitrary Contour Around a Moving Crack Tip.

The fixed coordinates are (X_1, X_2) and the moving coordinates attached to the crack tip are (x_1, x_2) where

$$x_i = X_i - vt\delta_{1i} \quad , \quad (i = 1,2). \tag{1}$$

For a given system of particles surrounding the crack tip the increment of irreversible energy pumped into the crack tip is given by the relation

$$-\Delta aG = \Delta E - \Delta U \tag{2}$$

where G is the rate at which energy is dissipated by the moving crack, ΔE is the increase in total energy, and ΔU is the work done on the system.

Referring to Figure 2, the system of particles to be considered is included in the area A_0 bounded by C and the area A_1 bounded by C_1 and C at time t. At time $t + \Delta t$ the same particles are bounded by C (enclosing A_0) and C and C_2 (enclosing A_2). Note that C_1 and C_2 are fixed contours and C is a moving contour. Then

$$\Delta U = \int_{C_1+C_2} \Delta u_i T_i ds \tag{3}$$

and

$$\Delta E = \int_{A_0} \xi(x_k, t+\Delta t) dA_0 - \int_{A_0} \xi(x_k, t) dA_0 + \int_{-C_2} \xi(X_k, t) v\Delta t dX_2$$
$$- \int_{C_1} \xi(X_k, t) v\Delta dX_2 + \int_{C_1+C_2} O(\Delta t^2) dX_2 \tag{4}$$

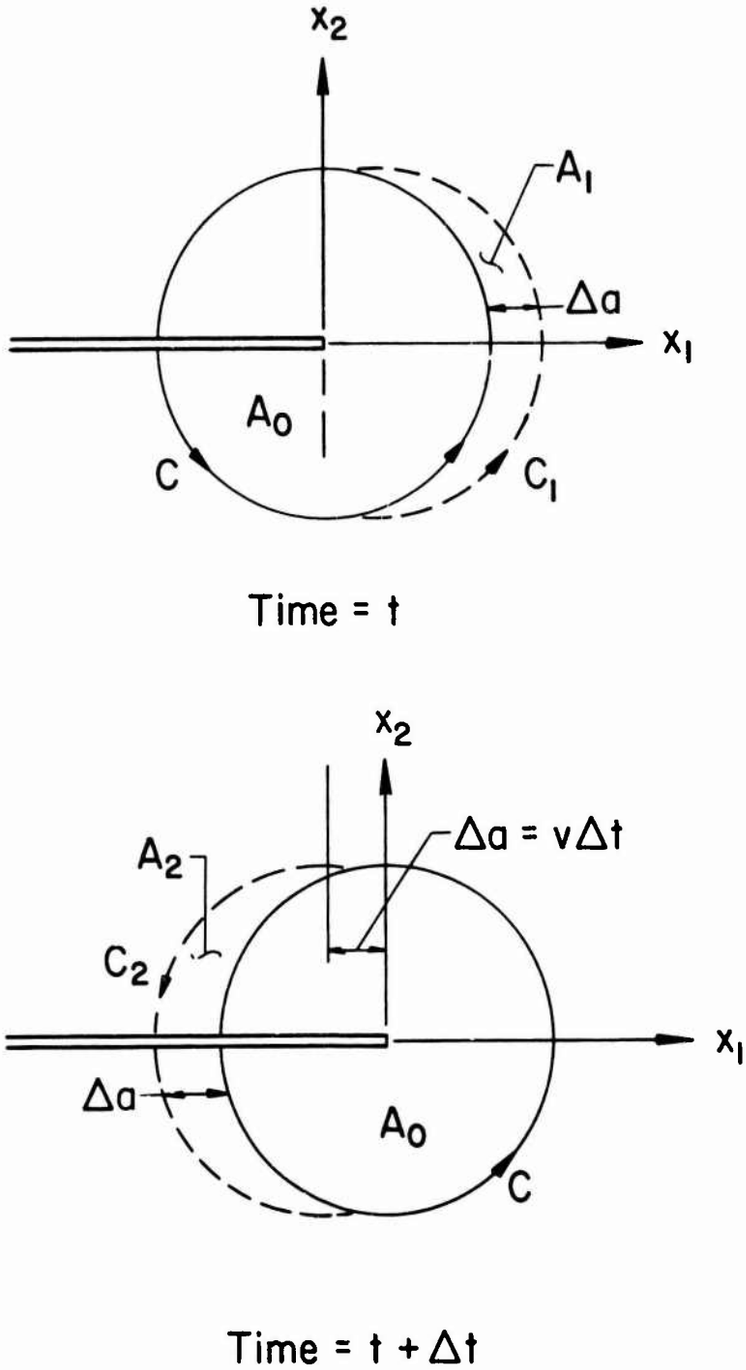

Figure 2. Incremental Motion of Crack Tip.

where

$$\xi = W + \frac{1}{2}\rho \frac{Du_i}{Dt}\frac{Du_i}{Dt} = W + \frac{1}{2}\rho \dot{u}_i \dot{u}_i \ . \tag{5}$$

Noting that $C_1 + C_2$ coincides with C in the limit and dividing through by Δt, the limit as $\Delta t \to 0$ is

$$-vG = \int_{A_0} \frac{\partial \xi}{\partial t} dx_1 dx_2 - \int_C \xi(x_k,t) v \delta_{2i} ds_i - \int_C \frac{Du_i}{Dt} T_i ds$$

or

$$vG + \int_{A_0} \frac{\partial \xi}{\partial t} dx_1 dx_2 = \int_C [\xi(x_k,t) v dx_2 + T_i u_i ds] \ . \tag{6}$$

2.2 STEADY STATE AND STATIC CASE

For the steady state case

$$\frac{\partial \xi}{\partial t} = 0$$

and

$$\frac{Du_i}{Dt} = \frac{\partial u_i}{\partial t} - v \frac{\partial u_i}{\partial x_1} = -v \frac{\partial u_i}{\partial x_1} \ . \tag{7}$$

Then

$$G_{s.s.} = \int_C [\xi^*(x_k) dx_2 - T_i \frac{\partial u_i}{\partial x_1} ds] \tag{8}$$

where

$$\xi^*(x_k) = W + \frac{1}{2}\rho v^2 \frac{\partial u_i}{\partial x_1}\frac{\partial u_i}{\partial x_1} \ . \tag{9}$$

For the static case, the energy release rate is also given by Eq. (8) with the kinetic energy term being zero. Thus,

$$G_{st} = \int_C [W dx_2 - T_i \frac{\partial u_i}{\partial x_1} ds] \ . \tag{10}$$

This result was given by Rice [12]. The integrals in Eqs. (8) and (10) are path independent, as shown by Sih [3] for Eq. (8).

2.3 BROBERG'S PROBLEM

For the case of a uniformly expanding crack of length 2vt, $\partial\xi/\partial t$ is not zero. However, making use of the displacement and stress solutions which are given in Appendix I for mode I opening, it may be shown that in the limit as the area enclosed by the contour is reduced to zero the following expression holds:

$$\lim_{C\to 0} \int_{A_0} \frac{\partial \xi}{\partial t} dA_0 = 0 \ . \tag{11}$$

Hence,

$$vG_I = \lim_{C\to 0} \int_C [v\xi(x_k,t)dx_2 - T_i v_i ds] \ . \tag{12}$$

Making use of Equations (5), (7), and (9), the preceding expression for G_I may be written in the form,

$$G_I = \lim_{C\to 0} \int_C [\xi^*(x_k)dx_2 - T_i \frac{\partial u_i}{\partial x_1} ds] +$$

$$+ \lim_{C\to 0} \frac{\rho}{2} \int_C \left[\frac{\partial u_i}{\partial t} \frac{\partial u_i}{\partial t} - 2v \frac{\partial u_i}{\partial t} \frac{\partial u_i}{\partial x_1} \right] ds$$

$$- \lim_{C\to 0} \frac{1}{v} \int_C T_i \frac{\partial u_i}{\partial t} ds \ . \tag{13}$$

As was the case for Equation (11), the second and third integrals on the right hand side of Equation (13) reduce to zero in the limit as $C\to 0$. Since Sih has shown that the remaining integral is path independent [3], the expression for G_I is the same as given in Equation (8) for the steady state case. Thus in terms of the function $F(s_1 s_2)$ which is defined for several cases of uniform crack extension in Appendix I, a general expression which is applicable to all cases of uniform elastic crack extension in mode I that are considered here may be written

$$\frac{G_I}{G_I^*} = \frac{4}{\kappa+1} s_1(1-s_2^2)[4s_1 s_2-(1+s_2^2)^2]F_1^2(s_1,s_2) \tag{14}$$

where

$$G_I^* = \lim_{v\to 0} G_I = \frac{\pi(\kappa+1)}{8\mu} k_1^2 \tag{15}$$

with k_1 being the corresponding static stress-intensity factor for the particular problem under consideration and with

$$\kappa = \begin{cases} 3-4\nu & \text{Plane Strain} \\ (3-\nu)(1+\nu), & \text{Plane Stress.} \end{cases} \tag{16}$$

2.4 PLASTIC ENERGY DISSIPATION

Consideration of the effects of ductility upon dynamic crack extension may be made by use of the Dugdale [13] hypothesis which is explained in detail in Section IV. For steady state problems where the plastic zone size remained fixed with time, the energy release rate (or plastic energy dissipation) may be calculated by direct application of Equation (8) to an equivalent elastic problem.

Consider, however, the motion of an expanding crack of length 2c where c is a function of time and with a thin Dugdale-type plastic zone located ahead of the crack tip. As shown by Atkinson [14] (see Section V) for uniform extension, this plastic zone must be expanding with time in order that the Dugdale hypothesis of finite stress at the end of the plastic zone be satisfied. Therefore, the results of the first part of this chapter cannot be used here even for the uniformly expanding crack since the contour C, which must enclose the entire region where energy dissipation takes place, was assumed to be fixed in shape and size. Obviously, an expanding plastic zone size would demand an expanding contour and therefore a separate analysis for this case is made here.

Figure 3 shows the configuation of the crack surface and plastic zone boundary at times t and $t+\Delta t$ during which time the crack edge extends by an amount $\Delta c = v(t)\Delta t$ and

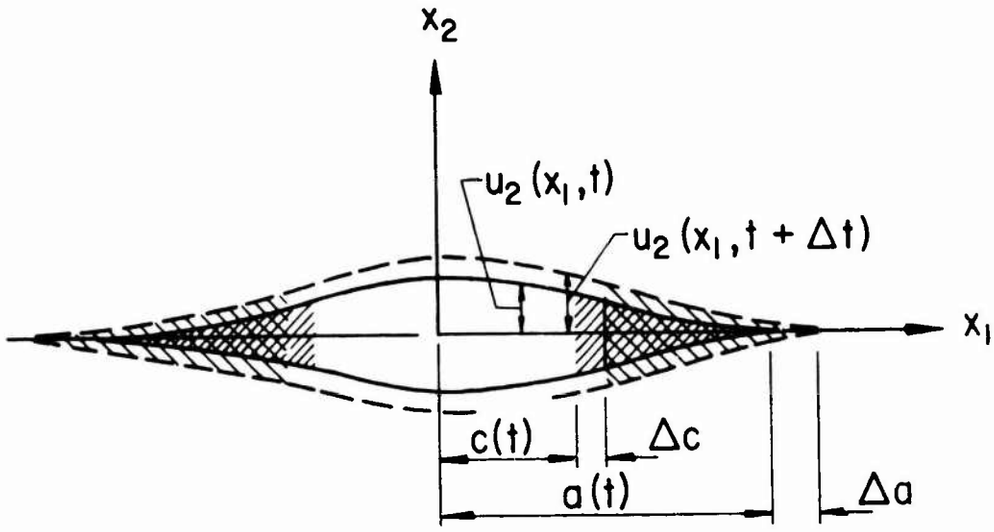

Figure 3. Change in Displacement of Crack Surface and Elastic-Plastic Interface over Increment of Time Δt.

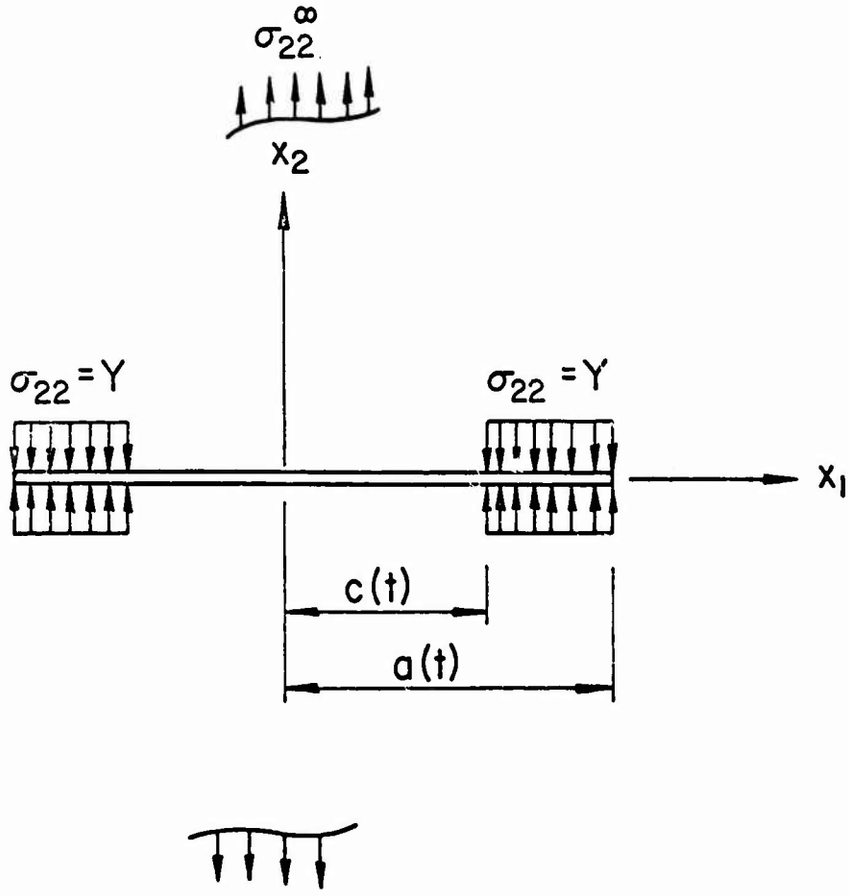

Figure 4. Geometry and Load Configuration for Equivalent Elastic Problem.

the plastic zone extends by an amount $\Delta a = \beta(t)\Delta t$ ($\Delta a \geq \Delta c$). The expression for the increment of energy released on the right-hand side of the crack is then equal to the plastic energy dissipated in the movement shown.

Recalling the assumption of a thin plastic strip, the elastic-plastic problem being considered may be converted to the elastic problem of a crack of length 2a with tensile stress equal to the yield stress Y of the material acting on the region $c \leq x \leq a$ of the crack surface (see Figure 4). The negative work done by these tractions is then equal to the plastic energy dissipation and, for the case of perfectly plastic material, where Y is constant, the resulting expression for energy released during the interval of time Δt is

$$G_I \Delta C = -\Delta U_p = 2Y \int_{x_1=c(t)}^{x_1=a(t)} \frac{\partial u_2}{\partial t} \Delta t \, dx_1 \tag{17}$$

where G_I is the energy release rate per unit crack extension, ΔU_p is the work done on the elastic plastic boundary, and u_2 is the displacement of the crack surface in the x_2-direction.

Now introduce the dimensionless time variable τ as

$$\tau = c_1 t \tag{18}$$

and normalize the crack velocity v and plastic zone velocity β with respect to c_1 so that the following normalized crack velocities are defined:

$$b(\tau) = \frac{v(t)}{c_1} \quad , \qquad \beta_0(\tau) = \frac{\beta(t)}{c_1} \; . \tag{19}$$

Then, the result in the limit as $\Delta t \to 0$ is

$$G_I b = 2Y \int_{x_1=c(\tau)}^{x_1=a(\tau)} \frac{\partial u_1}{\partial \tau} \, dx_1 \; . \tag{20}$$

The calculation of G_I for uniform crack extension, u, with b and β_0 constant, is carried out in Section V.

SECTION III

SUDDEN APPEARANCE OF A CRACK

The response of a solid medium to the sudden application of loads or the sudden appearance of geometric defects has engendered considerable interest in the past. However, it has been only recently that any consideration has been given to the propagation of transient elastic waves in bodies containing mechanical flaws or cracks. Due to the crack geometry this class of problems involves mixed edge conditions where both stress and displacement must be prescribed on a particular boundary. Such conditions can give rise to singular stresses.

An important case associated with the problem of projectile penetration is that of a crack appearing suddenly in a stressed medium. The associated disturbance due to the [illegible] may be studied in two separate regions: the local region near the crack edge (near-field) or the region close to the wave front propagating away from the crack (far-field). In fracture mechanics, much of the interest is centered on the near-field solution which describes the condition of possible crack extension. The far-field solution may be of use in determining the effects of the crack on other parts of the structure. The necessity of describing the two solutions separately is due to the adopted mathematical technique for solving crack problems which generally yields a tractable solution in only one of these regions.

A number of crack problems of this type have been solved for the case of anti-plane shear (see, for example, Kostrov [15]); however, the mathematical techniques employed are so far inapplicable to problems of in-plane loading. For in-plane loading, the only crack problem that has been solved so far is concerned with the case of a semi-infinite crack suddenly appearing in a stretched elastic plate. Maue [16] and Baker [17] have considered this problem using the Weiner-Hopf technique. The solution obtained is unbounded as $t \to \infty$ and does not permit meaningful comparison with a static case; however, the near-field stress solution is valid near the tip of a finite crack for the initial period of time before interaction with stress waves emanating from the other crack tip occurs.

In this section, the complete near-field solution to the problem of a finite line crack subjected to transient in-plane loading will be considered. The transient response of the material in the neighborhood of the crack tip will be obtained for the case of sudden application of self-equilibrating tractions to the crack surface. The crack is contained in an initially unstressed infinite elastic plate and is oriented as shown in Figure 5. For mathematical simplicity, the load is separable into a spatial and temporal function where the spatial function is even in x_1. Symmetry conditions then allow the problem to be solved in the upper plane only [18]. The special case where sudden uniform pressure, $\sigma H(t)$, is applied is treated in detail. Here,

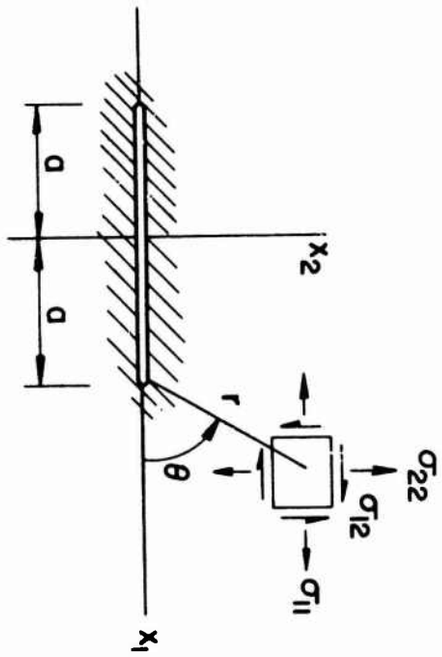

Self - Equilibrating Tractions

$q(x_1)\ f(t)$

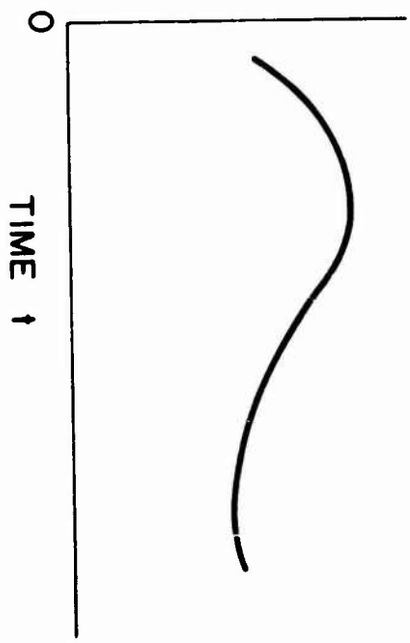

Figure 5. Crack Geometry and Stress Components.

H(t) is the Heaviside step function. The addition of this problem to the case of an infinite uncracked plate under uniform tensile stress σ corresponds to the problem of the sudden appearance of a crack in a stressed plate.

The analysis is done in two major steps. The problem is first formulated with the aid of Fourier and Laplace transforms and reduced to a Fredholm integral equation in terms of the Laplace transform variable. The Laplace transforms of the stress components are then inverted by a combination of numerical means and application of the Cagniard inversion technique.

3.1 FORMULATION OF PROBLEM

For plane elastodynamic problems, the displacement components may be expressed in terms of two scalar potentials, $\phi(x_1,x_2,t)$ and $\psi(x_1,x_2,t)$ so that

$$u_1 = -\frac{\partial\phi}{\partial x_1} + \frac{\partial\psi}{\partial x_2}$$

$$u_2 = -\frac{\partial\phi}{\partial x_2} - \frac{\partial\psi}{\partial x_1} \tag{21}$$

where ϕ and ψ satisfy the second-order partial differential equations

$$\nabla^2\phi = \frac{1}{c_1^2}\frac{\partial^2\phi}{\partial t^2} \quad , \quad \nabla^2\psi = \frac{1}{c_2^2}\frac{\partial^2\psi}{\partial t^2} \tag{22}$$

with ∇^2 being the Laplacian operator. The dilational and

shear wave velocities are, respectively,

$$c_1 = [(\lambda+2\mu)/\rho]^{\frac{1}{2}} \quad , \quad c_2 = (\mu/\rho)^{\frac{1}{2}} \tag{23}$$

where λ and μ are the Lamé constants.

Applying the strain displacement and constitutive equations for a homogeneous isotropic elastic media, the stresses may be written in terms of ϕ and ψ as,

$$\begin{aligned}
\sigma_{11} &= -\rho c_1^2 \nabla^2 \phi + 2\rho c_2^2 \frac{\partial}{\partial x_2}\left(\frac{\partial \psi}{\partial x_1} + \frac{\partial \phi}{\partial x_2}\right) \\
\sigma_{22} &= -\rho c_1^2 \nabla^2 \phi - 2\rho c_2^2 \frac{\partial}{\partial x_1}\left(\frac{\partial \psi}{\partial x_2} - \frac{\partial \phi}{\partial x_1}\right) \\
\sigma_{12} &= -\rho c_2^2 \left(\frac{\partial^2 \psi}{\partial x_1^2} - \frac{\partial^2 \psi}{\partial x_2^2} + 2\frac{\partial^2 \phi}{\partial x_1 \partial x_2}\right)
\end{aligned} \tag{24}$$

If the material is initially unstressed, the stress and displacement field due to sudden application of normal tractions to the crack surface may be found by solving the preceding field equations subject to zero initial conditions and the following boundary conditions at $x_2 = 0$:

$$\begin{aligned}
\sigma_{22}(x_1,0,t) &= -\sigma q(x_1) f(t) \quad , \quad \text{for } |x_1|<a \\
\sigma_{12}(x_1,0,t) &= 0 \quad , \quad \text{for } 0<|x_1|<\infty \\
u_2(x_1,0,t) &= 0 \quad , \quad \text{for } |x_1|>a \ .
\end{aligned} \tag{25}$$

In addition, the condition on displacement at infinity is

$$\lim_{x_1^2 + x_2^2 \to \infty} [u_1(x_1,x_2,t) \ , \ u_2(x_1,x_2,t)] = 0 \ .$$

The parameter σ is a constant with the dimension of stress and $q(x_1)$ is restricted to functions that are even in x_1; that is,

$$q(x_1) = q(-x_1) \ .$$

3.2 DUAL INTEGRAL EQUATIONS

Recalling that the initial conditions are zero, the Laplace transform may be applied to Equation (22) with the result

$$\nabla^2\phi^* = (p/c_1)^2\phi^* \quad , \quad \nabla^2\psi^* = (p/c_2)^2\psi^* \tag{26}$$

where the Laplace transform pair is defined by the equations:

$$f^*(p) = \int_0^\infty f(t)\exp(-pt)dt$$

$$f(t) = \frac{1}{2\pi i}\int_{Br} f^*(p)\exp(pt)dp$$

where the second integral is over the Bromwich path [19].

In order to reduce Equation (26) to ordinary differential equations, the Fourier cosine and sine transforms will be applied. The Fourier cosine transform pair is

$$\bar{f}(\alpha) = \int_0^\infty f(x_1)\cos(\alpha x_1)dx_1 \quad , \quad f(x_1) = \frac{2}{\pi}\int_0^\infty \bar{f}(\alpha)\cos(\alpha x_1)d\alpha$$

and the Fourier sine transform pair is

$$\hat{f}(\alpha) = \int_0^\infty f(x_1)\sin(\alpha x_1)dx_1 \ , \quad f(x_1) = \frac{2}{\pi}\int_0^\infty \hat{f}(\alpha)\sin(\alpha x_1)d\alpha \ .$$

The application of these transforms will depend on whether the function under consideration is even or odd in x_1.

By consideration of the symmetry properties of the boundary conditions, it can be shown that for the case considered here,

$$\phi(x_1,x_2,t) = \phi(-x_1,x_2,t) \ , \quad \psi(x_1,x_2,t) = -\psi(-x_1,x_2 t)$$

and the solution may be considered in the first quadrant of the plane.

Then, the Fourier cosine transform is applied to the function ϕ^* and the Fourier sine transform is applied to ψ^* in Equation (26), the result being,

$$\begin{aligned} &\frac{d^2\bar{\phi}^*}{dx_2^2} - [\alpha^2 + (p/c_1)^2]\bar{\phi}^* = 0 \\ &\frac{d^2\hat{\psi}^*}{dx_2^2} - [\alpha^2 + (p/c_2)^2]\hat{\psi}^* = 0 \ . \end{aligned} \tag{27}$$

Solutions to Equation (27) that satisfy the regularity conditions at infinity are

$$\begin{aligned} \bar{\phi}^* &= \frac{\pi}{2} A(\alpha,p)\exp(-\gamma_1 x_2) \\ \hat{\psi}^* &= \frac{\pi}{2} B(\alpha,p)\exp(-\gamma_2 x_2) \end{aligned} \tag{28}$$

provided the α-plane is cut so that

$$\sqrt{\alpha^2 + (p/c_j)^2} \geq 0 \qquad -\infty<\alpha<\infty \qquad (j = 1,2) \ .$$

The inverse Fourier transforms of Equation (28) are

$$\begin{aligned} \phi^* &= \int_0^\infty A(\alpha,p)\exp(-\gamma_1 x_2)\cos(\alpha x_1)d\alpha \\ \psi^* &= \int_0^\infty B(\alpha,p)\exp(-\gamma_2 x_2)\sin(\alpha x_1)d\alpha \ . \end{aligned} \tag{29}$$

The quantities γ_1 and γ_2 in Equations (28) and (29) are defined as

$$\gamma_1 = \sqrt{\alpha^2 + (p/c_1)^2} \quad , \quad \gamma_2 = \sqrt{\alpha^2 + (p/c_2)^2} \ .$$

By combining the Laplace transform of τ_{xy} with ϕ^* and ψ^*, the second boundary condition in Equation (25) may be expressed in the form,

$$\int_0^\infty \alpha\gamma_1 A(\alpha,p) - [\alpha^2 + \tfrac{1}{2}(p/c_2)^2]B(\alpha,p) \quad \sin(\alpha x_1)d\alpha = 0 \qquad 0 < |x_1| < \infty \ .$$

The preceding equation is satisfied for all x_1 by defining a new function $D(\alpha,p)$ such that

$$A(\alpha,p) = \frac{[\alpha^2 + \frac{1}{2}(p/c_2)^2]}{\gamma_1} D(\alpha,p) \ , \ B(\alpha,p) = \alpha D(\alpha,p) \ .$$

Then, referring to Equation (29), ϕ^* and ψ^* may be written as

$$\phi^* = \int_0^\infty \frac{1}{\gamma_1}\left(1 + \frac{1}{2\alpha^2 k^2}\right) D(\alpha,p)\exp(-\gamma_1 x_2)\cos(\alpha x_1)\alpha^2 d\alpha$$

$$\psi^* = \int_0^\infty D(\alpha,p)\exp(-\gamma_2 x_2)\sin(\alpha x_1)\alpha d\alpha \tag{30}$$

with the parameter k defined as,

$$k = c_2/p.$$

Finally, the first and third boundary conditions in Equation (25) may be applied by substitution of Equation (30) into the Laplace transforms of σ_{22} and u_2. The resulting set of dual integral equations is,

$$\int_0^\infty g(\alpha k)D(\alpha,p)\cos(\alpha x_1)\alpha d\alpha = \frac{\sigma q(x_1)f^*(p)}{\rho p^2}, \quad |x_1| < a$$

$$\int_0^\infty D(\alpha,p)\cos(\alpha x_1)d\alpha = 0 \quad , \quad |x_1| > a \tag{31}$$

where $f^*(p)$ is the Laplace transform of the function $f(t)$ in the first of Equation (25) and where

$$g(z) = 2z^2[1+(c_0/z)^2]^{-\frac{1}{2}}\left\{\left(1 + \frac{1}{2z^2}\right)^2 - \left(1 + \frac{1}{z^2}\right)^{\frac{1}{2}}[1+(c_0/z)^2]^{\frac{1}{2}}\right\}$$

with

$$c_0 = c_2/c_1.$$

In order to put the dual integral equations in a form amenable to solution, the first of Equation (31) is integrated

with respect to x_1 over the interval $(0,x_1)$. The result is

$$\int_0^\infty g(\alpha k)D(\alpha,p)\sin(\alpha x_1)d\alpha = \frac{\sigma Q(x_1)f^*(p)}{\rho p^2} \qquad |x_1|<a$$

$$\int_0^\infty D(\alpha,p)\cos(\alpha x_1)d\alpha = 0 \qquad |x_1|>a \tag{32}$$

where

$$Q(x_1) = \int_0^{x_1} q(s)ds \ .$$

Following the usual argument for solution of dual integral equations [20], a displacement related function $h^*(x_1,p)$ is defined by the equation,

$$h^*(x_1,p) = \frac{2}{\pi}\int_0^\infty D(\alpha,p)\cos(\alpha x_1)d\alpha \ . \tag{33}$$

Then, noting that the second of Equation (32) requires that $h^*(x_1,p)$ be zero for $|x_1|>a$, the Fourier inversion theorem leads to the expression

$$D(\alpha,p) = \int_0^a h^*(x_1,p)\cos(\alpha x_1)d\alpha \ . \tag{34}$$

The function $h^*(x_1,p)$ is to be constructed to possess the proper asymptotic behavior at the crack border, so that the near-field displacement is proportional to the square root of the distance from the crack edge. To this end, let

$$h^*(x_1,p) = \int_{x_1}^{a} \frac{U^*(\tau,p)\tau d\tau}{\sqrt{\tau^2-x_1^2}} \quad , \quad 0<x_1<a \, . \tag{35}$$

Substitution of Equation (35) into Equation (34) and application of the identity [21]

$$\int_0^{\tau} \frac{\cos(\alpha x_1)dx_1}{\sqrt{\tau^2-x_1^2}} = \frac{\pi}{2} J_0(\alpha\tau) \tag{36}$$

where J_0 denotes the zero order Bessel function of the first kind, leads to the expression

$$D(\alpha,p) = \frac{\pi}{2} \int_0^{a} U^*(\tau,p)J_0(\alpha\tau)\tau d\tau \, . \tag{37}$$

In order to rewrite the first of Equation (32) as an Abel's integral equation for $U^*(\tau,p)$ a function $W(\alpha k)$ is introduced such that,

$$W(\alpha k) = (1-c_0^2)-g(\alpha k) \, . \tag{38}$$

By virtue of Equations (37) and (38), the governing integral equation takes the form

$$(1-c_0^2) \int_0^{a} [U^*(\tau,p)\tau \int_0^{\infty} J_0(\alpha\tau)\sin(\alpha x_1)d\alpha]d\tau = \frac{2}{\pi} \frac{\sigma Q(x_1)f^*(p)}{\rho p^2} +$$

$$+ \int_0^{a} U^*(\tau,p)\tau \int_0^{\infty} W(\alpha k)J_0(\alpha\tau)\sin(\alpha x_1)d\alpha]d\tau \quad |x_1|<a \, . \tag{39}$$

Using the identity,

$$\int_0^\infty J_0(\alpha\tau)\sin(\alpha x_1)d\alpha = \begin{cases} 0 & 0<x_1<\tau \\ (x_1^2 - \tau^2)^{-\frac{1}{2}} & x_1>\tau \end{cases}$$

the desired form of Abel's integral equation [22] is obtained.

$$(1-c_0^2)\int_0^{x_1} \frac{U^*(\tau,p)\tau d\tau}{\sqrt{x_1^2-\tau^2}} = \frac{2}{\pi}\frac{\sigma Q(x_1)f^*(p)}{\rho p^2}$$

$$+ \int_0^a [U^*(\tau,p)\tau \int_0^\infty W(\alpha k)J_0(\alpha\tau)\sin(\alpha x_1)d\alpha]d\tau \qquad |x_1|<a .$$

Inversion of the preceding equation yields

$$(1-c_0^2)U^*(\tau,p) = \frac{2}{\pi}\int_0^\tau \frac{1}{\sqrt{\tau^2-x_1^2}} \left\{\frac{2}{\pi}\frac{\sigma q(x_1)f^*(p)}{\rho p^2}\right.$$

$$\left. + \int_0^a [U^*(\zeta,p)\zeta \int_0^\infty W(\alpha k)J_0(\alpha\zeta)\cos(\alpha x_1)\alpha d\alpha]d\zeta\right\} dx_1$$

$$\tau < a . \qquad (40)$$

Now, introduce the non-dimensional variables

$$\xi = \tau/a , \qquad \eta = \zeta/a , \quad s = \alpha a \quad , \quad z = x_1/a$$

and define

$$\kappa = k/a \qquad\qquad \beta(z) = W(za)$$

$$\Lambda^*(\xi,\kappa) = \frac{\pi}{2}(1-c_0^2)\frac{\rho p^2\sqrt{\xi}\, U^*(\xi a,p)}{\sigma f^*(p)} .$$

Then, making use of Equation (36), Equation (40) may be written in the form of a Fredholm integral equation of the second kind.

$$\Lambda^*(\xi,\kappa)-\int_0^1 \Lambda^*(\eta,\kappa)K(\xi,\eta)d\eta = \frac{2}{\pi}\sqrt{\xi}\int_0^{\xi}\frac{\beta(z)dz}{\sqrt{\xi^2-z^2}} \tag{41}$$

whose kernal, being symmetric in ξ and η, is

$$K(\xi,\eta) = \frac{\sqrt{\xi\eta}}{(1-c_0^2)}\int_0^{\infty} sW(s\kappa)J_0(s\eta)J_0(s\xi)ds, \quad 0\leq\xi\leq 1,\ 0\leq\eta\leq 1 .$$

For rapid convergence of the infinite integral, define a function d(z) as

$$d(z) = W(z) + \frac{H}{z^2+E^2}$$

where, in order that d(z) be of order $(z)^{-6}$ for large z, H and E^2 are chosen as

$$H = \frac{1}{4}(3c_0^4 - 4c_0^2 + 3)$$

$$E^2 = \frac{[5c_0^6 - 6c_0^4 + 2c_0^2 + 1]}{8H} .$$

Since

$$\int_0^{\infty}\frac{H}{(\alpha\kappa)^2+E^2}J_0(s\eta)J_0(s\xi)sds = \frac{H}{\kappa^2}I_0\left(\frac{E\xi}{\kappa}\right)K_0\left(\frac{E\xi}{\kappa}\right), \quad 0<\xi\leq\eta ,$$

the expression for the kernal in the Fredholm integral equation becomes

$$K(\xi,\eta) = \frac{\sqrt{\xi\eta}}{(1-c_0^2)} \left[-\frac{H}{\kappa^2} I_0\left(\frac{\xi E}{\kappa}\right) K_0\left(\frac{\eta E}{\kappa}\right) + \int_0^\infty s\,d(s\kappa) J_0(s\eta) J_0(s\xi)\,ds \right]_{0<\xi\leq\eta}$$

where I_0 and K_0 are the zero-order modified Bessel's functions of the first and second kind respectively.

Making use of Equation (37) and the definition of Λ^* the unknown function $D(\alpha,p)$ may be written in terms of the solution to the Fredholm integral equation as,

$$D(\alpha,p) = \frac{\sigma a^2 f^*(p)}{(1-c_0^2)\rho p^2} \int_0^1 \left[\frac{\Lambda^*(\xi,\kappa)}{\sqrt{\xi}}\right] J_0(\alpha a\xi)\xi\,d\xi \ .$$

This expression may be integrated by parts with the result

$$D(\alpha,p) = \frac{\sigma a f^*(p)}{(1-c_0^2)\rho p^2 \alpha} \left\{ \Lambda^*(1,\kappa) J_1(\alpha a) - \int_0^1 \frac{d}{d\xi}\left[\frac{\Lambda^*(\xi,\kappa)}{\sqrt{\xi}}\right] J_1(\alpha a\xi)\xi\,d\xi \right\} \tag{42}$$

from which the stresses and displacements may be determined.

3.3 TIME DEPENDENT STRESS FIELD

The integral expressions for the Laplace transforms of the potentials ϕ and ψ are now completely determined and, making use of Equation (24), corresponding expressions for the Laplace transforms of the dynamic stresses may be obtained. It remains then to take the inverse Laplace transforms. This may be accomplished by applying the Cagniard-DeHoop

inversion technique [8, 23]. Due to the complexity of calculation, the detailed procedure will be given only for the first stress invariant, $\sigma_{11} + \sigma_{22}$.

From Equations (24) and (26) the Laplace transform of $\sigma_{11} + \sigma_{22}$ is

$$\sigma^*_{11} + \sigma^*_{22} = -2\rho p^2(1-c_0^2)\phi^* \tag{43}$$

The part of the solution of interest here is the singular solution near the crack tip. For this portion of the solution it is sufficient that only the first term on the right hand side of Equation (42) be retained. The integral expression in $D(\alpha,p)$ is associated with terms that remain finite at the crack tip.

Putting ϕ^* in Equation (30) into Equation (43), the near-field solution for $\sigma_{11} + \sigma_{12}$ in the transformed plane is

$$\sigma^*_{11} + \sigma^*_{22} = -2\sigma a f^*(p)\Lambda^*(1,\kappa) \int_0^\infty \frac{1}{\alpha\gamma_1} [\alpha^2 + \frac{1}{2}(p/c_2)^2]$$

$$\cdot\, J_1(\alpha a)\exp(-\gamma_1 x_2)\cos(\alpha x_1)d\alpha\,. \tag{44}$$

Changing the variable of integration to $\alpha = wp$ and noting that J (awp) is an odd function with respect to w, Equation (44) becomes

$$\sigma^*_{11} + \sigma^*_{22} = -\sigma a f^*(p)\Lambda^*(1,\kappa)p \int_{-a}^{\infty} T(w)J_1(apw)\exp[-p(\sqrt{w^2+c_1^{-2}}x_2$$

$$- iwx_1)]dw$$

in which T(w) stands for

$$T(w) = \frac{w^2 + (1/2c_2^2)}{w\sqrt{w^2+(1/c_1^2)}} .$$

Making use of the identity [21],

$$J_1(x) = \frac{i}{\pi}\int_0^{\pi} \exp(-ix\cos\omega)\cos(\omega)d\omega$$

Equation (44) further simplifies to

$$\sigma_{11}^* + \sigma_{22}^* = -\frac{ia\sigma p}{\pi} f^*(p)\Lambda^*(1,\kappa)\int_0^{\pi}\cos(\omega)d\omega\left\{\int_{-\infty}^{\infty} T(w) \cdot \exp[-p(\sqrt{w^2+c_1^{-2}x_2}-iwX)]\right\} dw . \qquad (45)$$

The variable X is given as

$$X = x_1 - a\cos\omega .$$

To evaluate Equation (45), consider first the function I^* defined by the relation

$$I^* = \int_0^{\pi}\cos\omega d\omega \int_{-\infty}^{\infty} T(w)\exp[-p(\sqrt{w^2+c_1^{-2}}x_2 - iwX)]dw . \qquad (46)$$

This function is in a form suitable for evaluation through the Cagniard-DeHoop method. The objective then is to transform the integral on the right-hand side of Equation (46) into a recognizable Laplace transform. This may be done by making the change in variables,

$$\tau = \sqrt{w^2 + c_1^{-2}}\, x_2 - iwX .$$

Solving for w as a function of τ yields

$$w = \pm\sqrt{\tau^2 - (R/c_1)^2}\,\frac{x_2}{R^2} + \frac{iX\tau}{R^2} \tag{47}$$

in which $R^2 = X^2 + y^2$.

The remainder of the procedure consists of treating w as a complex variable and locating a path in the w-plane along which τ is a positive number. Referring to Figure 6 and noting that the integrand in Equation (46) possesses branch points at $\pm ic_1$, cuts are made in the w-plane as shown in order that the function $\sqrt{w^2+(1/c_1)^2}$ be single valued and have a real part that is positive everywhere in the w-plane. If τ is restricted to real non-negative values, Equation (47) is the equation of a hyperbola in the w-plane. If $X>0$ ($X<0$) the hyperbola will be in the upper (lower) half of the w-plane. The path of integration in Equation (46) can be converted from the real axis to the aforementioned hyperbola by making use of the Cauchy integral theorem and Jordan's Lemma. Thus, after changing the variable of integration to τ by means of Equation (47), it is found that

$$I^* = \int_0^{\pi} \cos\omega d\omega \int_{R/c_1}^{\infty} [T(w^+)\,\frac{dw^+}{d\tau} - T(w^-)\,\frac{dw^-}{d\tau}]\exp(-p\tau)d\tau \tag{48}$$

where the (+) and (-) superscripts refer to the right- (left-)

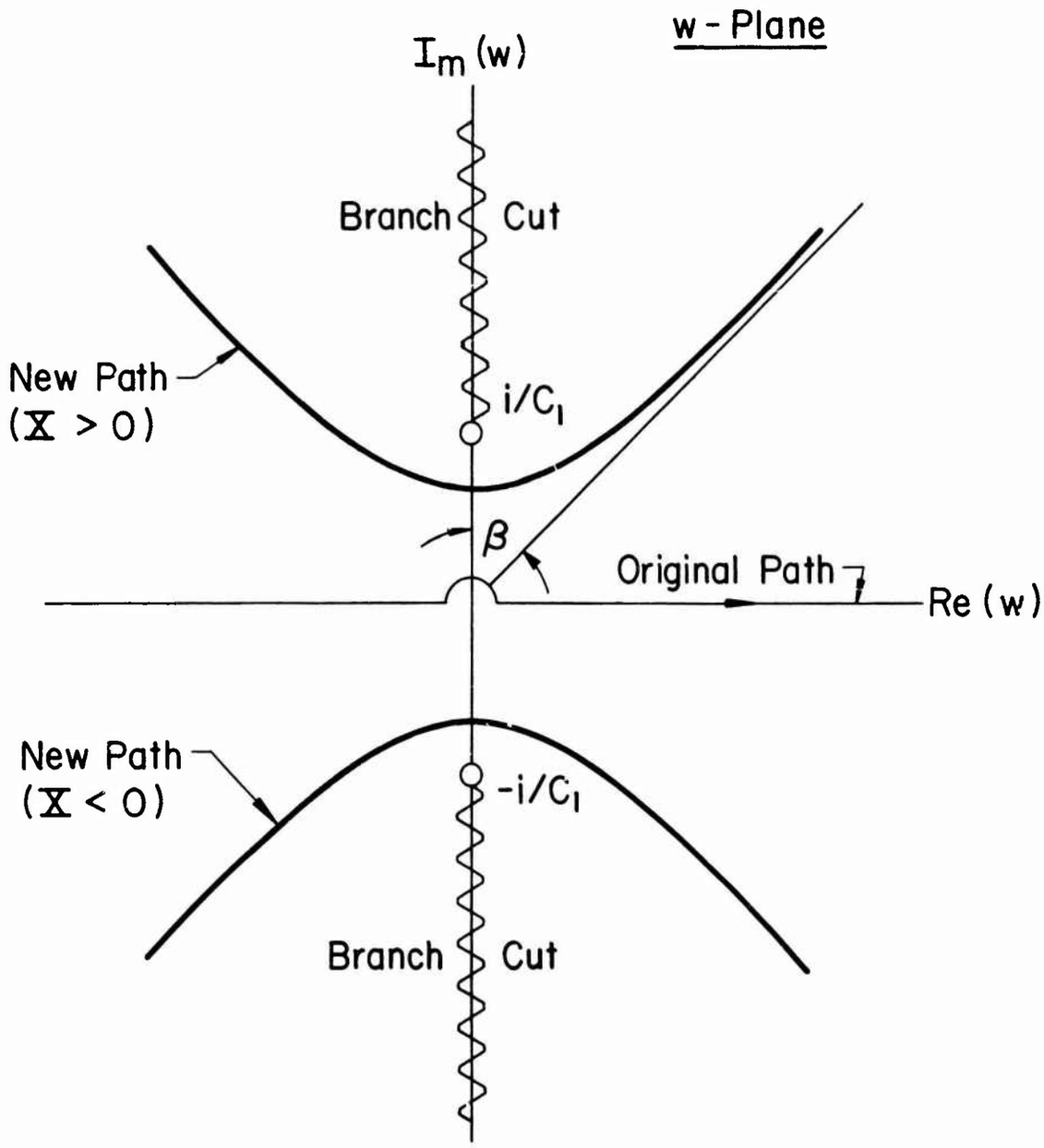

Figure 6. Path of Integration in w-plane.

hand legs of the hyperbola. Noting that the inner integral is in the form of a Laplace transform it is a matter of inspection to write the inverse Laplace transform of I^* as,

$$I\ (t) = \int_0^{\pi} H(t-\frac{R}{c_1})[T(w^+)\ \frac{dw^+}{dt} - T(w^-)\ \frac{dw^-}{dt}]\cos\omega d\omega \qquad (49)$$

where H(t) is the Heaviside step function. Referring to Equations (45) and (46) and making use of the convolution theorem for the Laplace transform, the stress invariant is obtained to be

$$\sigma_{11}+\sigma_{22} = -\frac{ia\sigma}{\pi}\int_0^t m(t-\tau)I(\tau)d\tau \qquad (50)$$

where

$$m(t) = L^{-1}[pf^*(p)\Lambda^*(1,\kappa)] \qquad (51)$$

with L^{-1} being the inverse Laplace transform operator.

In order to determine $\sigma_{11}+\sigma_{22}$ in the region near the crack tip it is necessary to extract the singular portion of I(t) from Equation (49). Without going into mathematical details, it is easy to show that, as long as c_2t is sufficiently greater than r, the radial distance measured from the crack tip, I is independent of time, i.e.,

$$I = -\frac{i}{a}\left[\int_{-a}^{a}\frac{qdq}{(q-z)\sqrt{a^2-q^2}} + \int_{-a}^{a}\frac{qdq}{(q-\bar{z})\sqrt{a^2-q^2}}\right]$$

with

$$z = x_1 + ix_2 \quad , \quad \bar{z} = x_1 - ix_2$$

and where the transformation of variable,

$$q = a\cos\omega$$

has been made.

Making use of Chapter 4 of Muskhelishvilli [24], the evaluation of the above integrals near the crack tip leads to the following expression for the singular portion of I,

$$I = \frac{2\pi i}{\sqrt{2ar}} \cos(\theta/2) + \cdots$$

where r and θ are polar coordinates with the origin attached to the crack tip as shown in Figure 7.

Then, referring to Equation 50, it follows that the near field solution for the stress invariant is

$$\sigma_{11} + \sigma_{22} = \frac{2\sigma\sqrt{a}}{\sqrt{2r}} M(t)\cos(\theta/2) + \cdots \tag{52}$$

where

$$M(t) = \int_0^t m(t)dt \ . \tag{53}$$

In a manner analagous to the static theory of brittle fracture, a dynamic stress intensity factor, $k_1(t)$ may be defined [3]

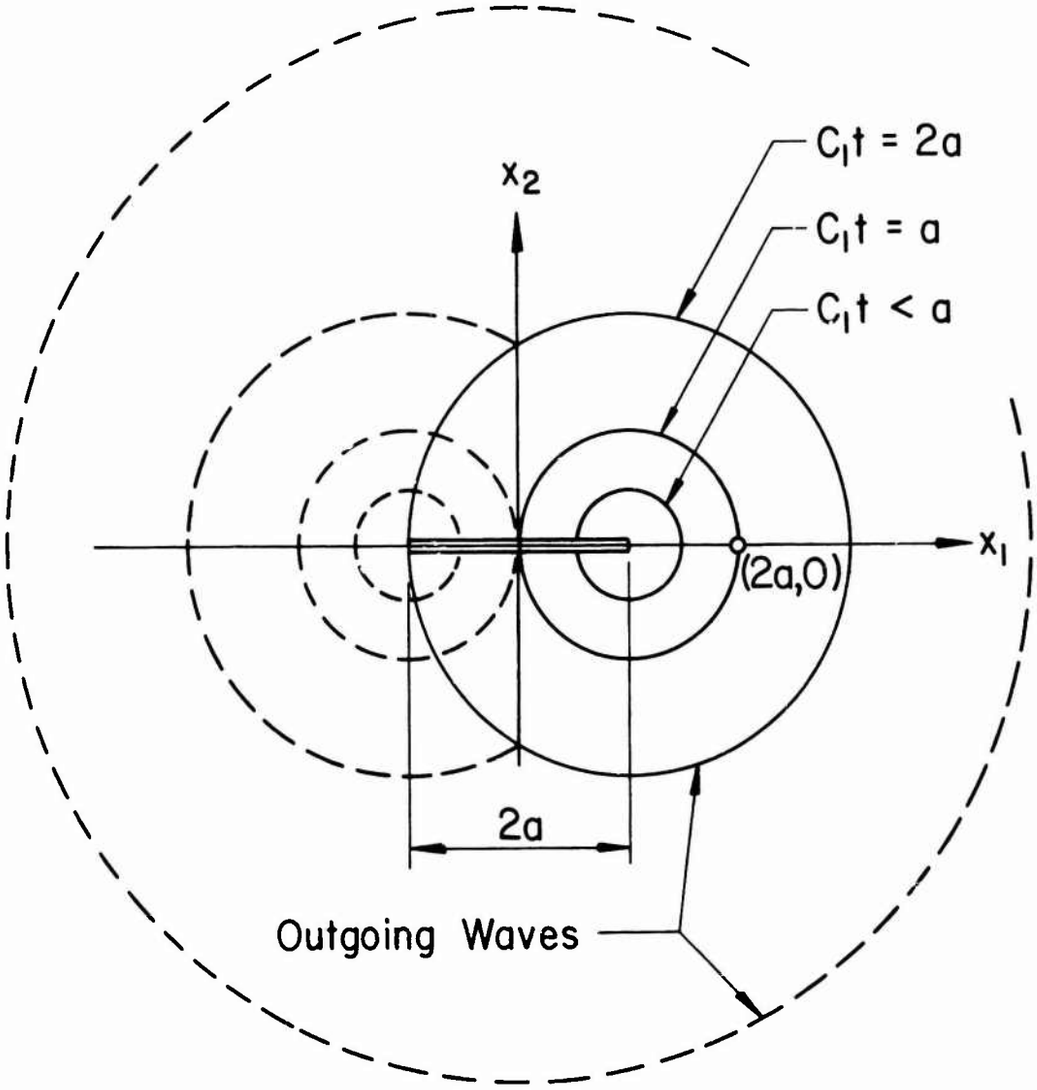

Figure 7. Wave Fronts Emanating from Crack Tips.

$$k_1(t) = M(t) \quad a \; . \tag{54}$$

With this definition the individual stress components may be evaluated, the result being

$$\sigma_{11} = \frac{k_1(t)}{\sqrt{2r}} \cos(\theta/2)[1-\sin(\theta/2)\sin(3\theta/2)] + \cdots$$

$$\sigma_{22} = \frac{k_1(t)}{\sqrt{2r}} \cos(\theta/2)[1+\sin(\theta/2)\sin(3\theta/2)] + \cdots$$

$$\sigma_{12} = \frac{k_1(t)}{\sqrt{2r}} \cos(\theta/2)\sin(\theta/2)\cos(3\theta/2) + \cdots \tag{55}$$

Thus, the stress field near the crack tip has the same spatial distribution for the dynamic case as for the static case the only difference being that the intensity of the field is a function of time. The time dependent stress-intensity factor $k_1(t)$ is related to the function m(t) which, noting Equation (51) depends ultimately on the function $\Lambda^*(1,\kappa)$. Thus, in order to obtain the stress-intensity factor for a given time dependent load applied to the crack surface, it is necessary to first numerically solve the integral Equation (41) for $\Lambda^*(1,\kappa)$ for various values of the Laplace transform variable p. Inversion of the Laplace transform numerically then enables the evaluation of M(t) and thus $k_1(t)$. This procedure is described in Appendix II.

Numerical results have been obtained for the case of a uniform load σ suddenly applied to the crack surface. That

is, $\sigma q(x_1)$ is a constant, and $f(t)$ is the Heaviside step function $H(t)$. By superposition, this type of loading corresponds to the sudden appearance of a crack in a stressed plate. The solution to the Fredholm integral equation, $A^*(1,\kappa)$ for this case is plotted in Figure 8. In Figure 9 the dynamic stress-intensity factor, $k_1(t)$, normalized with respect to the corresponding static value $\sigma\sqrt{a}$, is plotted as a function of c_2t/a. The ratio of shear wave speed, c_2, to dilatational speed c_1 that was used is 0.542 the value for steel. The significant feature of the solution is that the stress-intensity factor reaches a peak greater than the static value and subsequently oscillates about that value with decreasing amplitude until, in the limit as $t\to\infty$, $k_1 = \sigma\sqrt{a}$. When k_1 reaches its maximum value, c_2t/a is approximately equal to 3.0. For a crack where a is equal to one inch, this corresponds to an elapsed time of 2.4×10^{-5} seconds.

The method used here to determine the asymptotic behavior of the near-field stress solution requires only that the stress wave boundary be well beyond the region of interest. Thus, if the stress field is to be valid within a distance ε of the crack tip, the condition on the time elapsed is $c_2t \gg \varepsilon$. As long as ε is kept small enough, the solution is valid for all time (except very near $t = 0$). This condition on ε is, of course, in addition to the usual static restriction that $\varepsilon \ll a$.

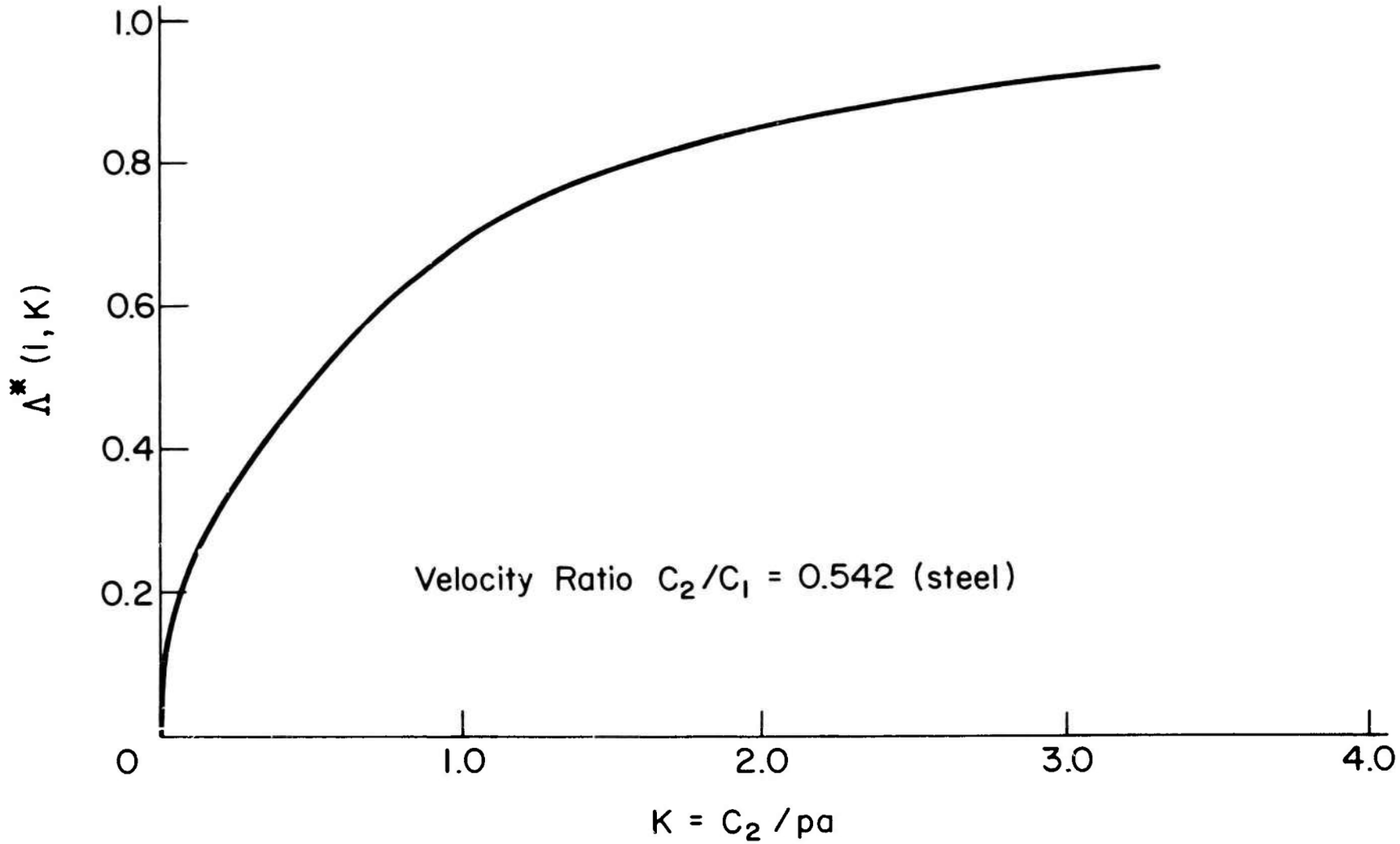

Figure 8. Solution to the Fredholm Integral Equation.

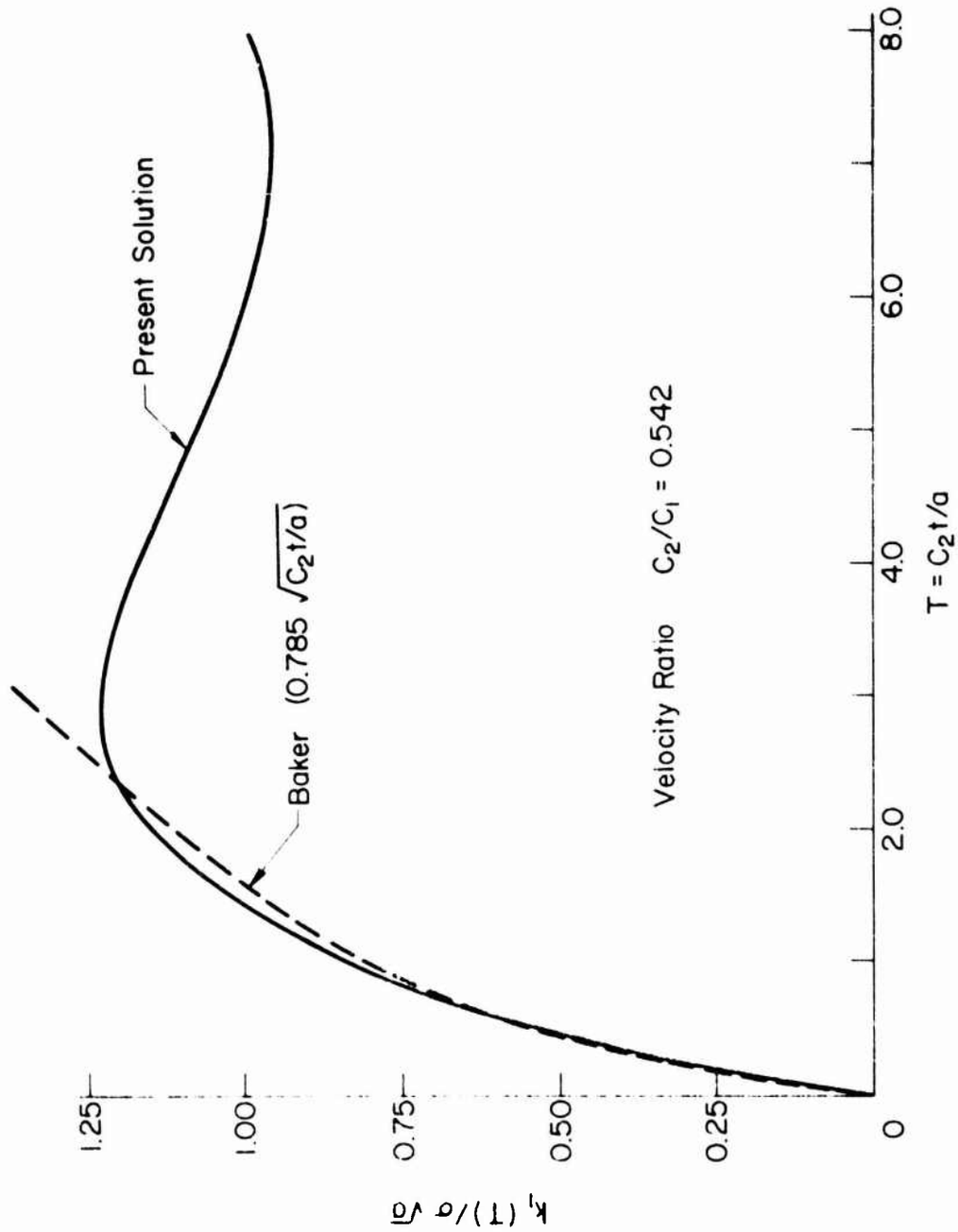

Figure 9. Dynamic Stress-Intensity Factor.

SECTION IV

PLASTICITY MODELS OF STEADY STATE CRACK EXTENSION

It is well known that upon reaching a certain critical stress or strain level the material in a region local to the crack tip will separate, causing crack propagation in a manner determined by the character of the stress field caused by impact and the structure of the target material. In materials without a substantial amount of yielding, the crack will normally start its motion abruptly and then very quickly settle down to a uniform speed. To estimate the amount of energy carried by a running crack, it is essential to have a mathematical description of the stress state near the crack. This is important in determining the condition required for cessation of crack motion.

For static problems, plasticity effects have been introduced into fracture analysis with a satisfactory amount of success (see a review article by Rice [12] for example). However, very little analysis has been done which deals with plastic behavior of material in the neighborhood of propagating cracks. For the few elastic solutions to dynamic crack problems which exist, the introduction of plastic effects causes complexities which, with the exception of the Dugdale model, have been beyond resolution.

The elastic crack propagation problems that have been studied are in two basic configurations. The solutions of

Yoffé [25] and Craggs [26] are representative of the first type (steady state). Yoffé considered the problem of a crack of fixed length moving through an infinite elastic continuum with a constant velocity. Craggs considered a similar problem where a semi-infinite crack propagates at a constant velocity and upon which tractions are applied to a segment of the surface which moves with the crack tip.

Broberg's [11] analysis of the physically more realistic configuration of a crack whose tips are expanding away from the origin at a constant rate is representative of the second type. The solution obtained by Broberg was also obtained by Craggs [27] who made use of the dynamic similarity possessed by solution.

4.1 THE DUGDALE MODEL

One available tool for extension of these configurations to include plastic behavior is the Dugdale [13] model. The Dugdale hypothesis, proposed for the case of plane stress yielding ahead of the crack tips, postulates that the yielded zone is a narrow region in the plane of the crack (see Figure 10). For a stationary crack of length 2c, the length of this zone is calculated by solving the elastic problems of a crack of length 2a with remotely applied tensile stress P and with tensile stress Y distributed over a length (a-c) of the crack which represents the boundary of the plastic zone (see Figure 11). A relationship between the geometry of the crack and plastic zone, the applied load, and the

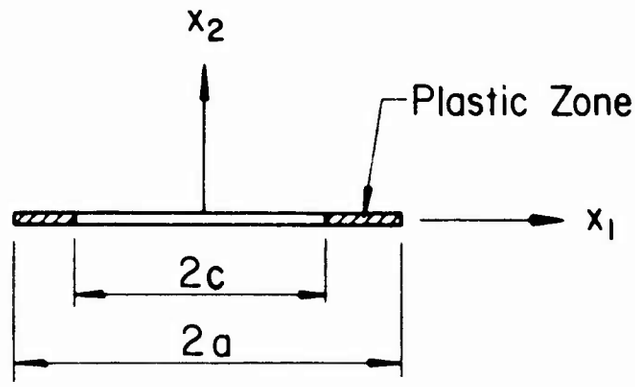

Figure 10. Line Crack with Dugdale Plastic Zone.

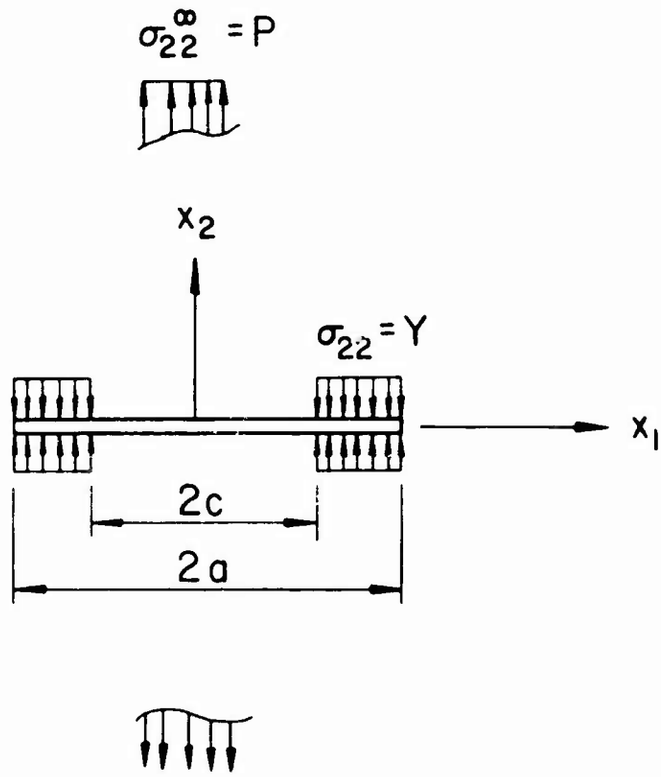

Figure 11. Equivalent Elastic Problem for Line Crack with Dugdale Plastic Zone.

yield stress Y is obtained through the requirement that stress be finite at the end of the plastic zone. The expression thus obtained is

$$\frac{c}{a} = \cos\left(\frac{\pi}{2}\frac{P}{Y}\right) . \tag{56}$$

This result was compared favorably with experimental measurements by Dugdale.

Subsequently, the Dugdale model has been incorporated into the case of a propagating semi-infinite crack by Goodier and Field [28], the Yoffé model by Kanninen et al [29], and the Broberg model by Atkinson [14]. In this section and Section V, these models will be examined with special attention directed toward the energy dissipation associated with each.

4.2 STEADY STATE CRACK PROPAGATION PROBLEMS

For steady state problems, with a disturbance moving to the right with velocity v in an infinite or semi-infinite medium, the Galilean transformation of coordinates, $x_i = X_i - vt\delta_{1i}$, allows the reduction of the number of independent variables from three to two. Thus, many of the powerful tools of two-dimensional analysis may be brought to bear on the problem. In particular, the complex variable technique of Muskhelishvilli is of great use in dealing with steady state crack propagation problems (see References [30], [31], and [32]). Thus, for a crack moving with velocity v, the stress

components of dynamic plane elasticity may be expressed in terms of two functions [31], $\Phi_j(z_j)$, (j=1,2), of the complex variables z_j as

$$\sigma_{11} = -2\mathrm{Re}[s_1^2 + \tfrac{1}{2}(1-s_2^2)\Phi_1(z_1) + \tfrac{1}{2}(1+s_2^2)\Phi_2(z_2)] \qquad (57)$$

$$\sigma_{22} = (1+s_2^2)\mathrm{Re}[\Phi_1(z_1) + \Phi_2(z_2)] \qquad (58)$$

$$\sigma_{12} = 2\mathrm{Im}[s_1\Phi_1(z_1) + \frac{(1+s_2^2)}{4s_2^2}\Phi_2(z_2)] \qquad (59)$$

where s_1 and s_2 are defined in Appendix I and,

$$z_j = x_1 + is_jx_2 \quad , \quad j = 1,2 \qquad (60)$$

with (x_1,x_2) being the coordinates in a frame of reference attached to the crack.

Similarly, the displacement field is

$$u_1 = -\frac{1}{\mu}\mathrm{Re}[\phi_1(z_1) + \tfrac{1}{2}(1+s_2^2)\phi_2(z_2)] \qquad (61)$$

$$u_2 = \frac{1}{\mu}\mathrm{Im}[s_1\phi_1(z_1) + \frac{1}{2}\left(\frac{1+s_2^2}{s_2}\right)\phi_2(z_2)] \qquad (62)$$

in which

$$\phi_j(z_j) = \int \Phi_j(z_j)dz_j \quad , \quad j = 1,2 . \qquad (63)$$

Due to simplicity of analysis then, most crack propagation problems that have been solved are steady state. The

two examples considered in this section are a semi-infinite crack with self-equilibrating concentrated loads Q applied at a fixed distance c from the crack tip and a finite crack of fixed length 2c. Both cracks propagate with constant velocity v.

4.3 SEMI-INFINITE CRACK

Considered here is the case of a semi-infinite crack whose motion is maintained by concentrated loads, Q, at a distance c from the crack tip. The geometry is shown for the elastic case in Figure 12 and for the plastic case in Figure 13.

The stresses and displacements for the elastic model may be obtained from Appendix I. Making use of Equation (14), the elastic energy release rate for plane stress is

$$\frac{G_I}{G_I^*} = \frac{(1+\nu)s_1(1-s_2^2)}{4s_1s_2 - (1+s_2^2)^2} \tag{64}$$

where G_I^* is the corresponding static value of the energy release rate and s_j $(j=1,2)$ is defined by Equation (I-6). For the semi-infinite model G_I^* is

$$G_I^* = \lim_{v\to 0} G_I = \frac{Q^2}{\pi\mu c(1+\nu)} . \tag{65}$$

The ratio G_I/G_I^* is plotted in Figure 18. This result is also valid for the case of the fixed length finite crack (with appropriate change in G_I^*).

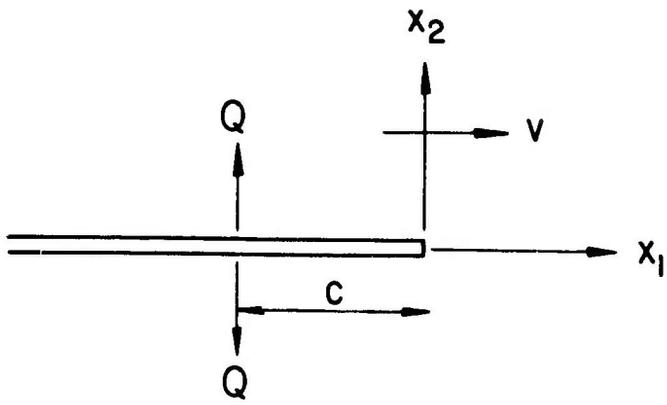

Figure 12. Semi-infinite Crack Loaded with Concentrated Forces.

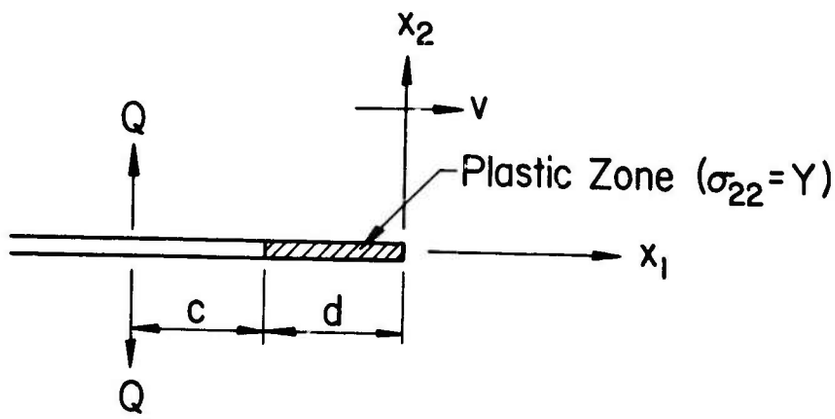

Figure 13. Semi-Infinite Crack with Dugdale Plastic Zone.

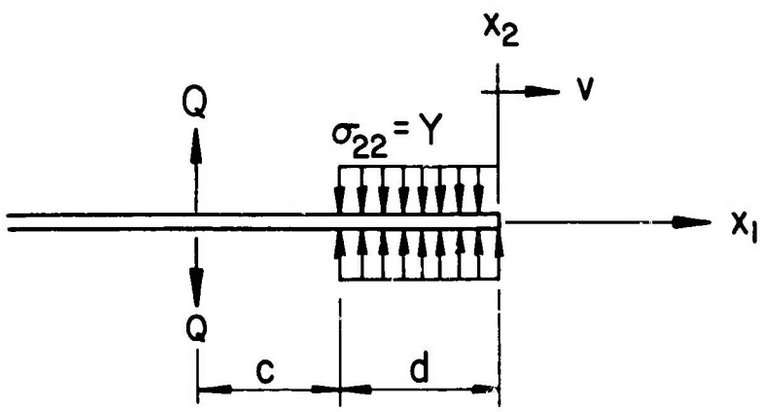

Figure 14. Equivalent Elastic Problem for Semi-Infinite Crack.

Using the Dugdale hypothesis a thin plastic zone ahead of the crack may be represented by an extension of the crack by a length equal to that of the plastic zone. Over this added increment of crack length tensile stress, $\sigma_{22} = Y$ equal to the yield strength of the material is applied. This is shown in Figure 14.

The incorporation of plasticity into the semi-infinite model may then be accomplished by direct application of the elastic solution as follows. The solution to the elastic problem with the coordinate system attached to the crack tip, as shown in Figure 12, has been derived by Sih [32], where the stress functions introduced in sub-section 4.1 are

$$\Phi_j(z_j) = -g_j(s_1,s_2)Q\sqrt{c/z_j}\ \left(\frac{1}{z_j+c}\right) \tag{66}$$

with the functions $g_j(s_1,s_2)$ being

$$g_1(s_1,s_2) = \frac{(1+s_2^2)}{\pi[4s_1s_2-(1+s_2^2)^2]} \tag{67}$$

$$g_2(s_1,s_2) = -\frac{4s_1s_2}{\pi(1+s_2^2)[4s_1s_2-(1+s_2^2)^2]}\ . \tag{68}$$

The corresponding displacement functions are, through Equation (63),

$$\phi_j(z_j) = ig_j(s_1,s_2)Q\ell n\left(\frac{i\sqrt{z_j}+\sqrt{c}}{i\sqrt{z_j}-\sqrt{c}}\right). \tag{69}$$

The preceding equations represent a fundamental solution in that they may be used to construct the solution for an arbitrary distributed load on the crack surface. For the problem of interest here, it is necessary to find the solution when uniform tractions of intensity p are applied to the segment of the crack lying between $x_1 = -d$ and $x_1 = 0$. That is, let

$$Q = pd\xi \qquad \text{and} \qquad c = -\xi \tag{70}$$

and integrate Equation (69) over the interval $-d \leq \xi \leq 0$, the result being

$$\phi_j(z_j) = -p\sqrt{d}\; g_j(s_1,s_2)\left\{2\sqrt{z_j} - \frac{i}{\sqrt{d}}\,(d+z_j)\ln\left(\frac{i\sqrt{z_j} + \sqrt{d}}{i\sqrt{z_j} - \sqrt{d}}\right)\right\} . \tag{71}$$

The stress functions $\Phi_j(z_j)$, upon differentiation of Eqs. (71) are found to be

$$\phi_j(z_j) = -pg_j(s_1,s_2)\left\{2\sqrt{d/z_j} - i\ln\left(\frac{i\sqrt{z_j} + \sqrt{d}}{i\sqrt{z_j} - \sqrt{d}}\right)\right\} \tag{72}$$

The solution to the elastic-plastic problem, where the loads Q are at a distance c from the physical crack tip and where the plastic zone extends a distance d beyond the crack tip may now be obtained by the principle of superposition (see Figure 14). That is, replace c by c+d in Equation (66), let p = -Y, where Y is the yield stress, in Equation (72), and the stress function for the elastic-plastic problem is equal

to the sum of Equations (66) and (72). The displacement function is obtained in the same manner. In order to satisfy the Dugdale hypothesis of finite stress at $x_1 = 0$, consider the resultant expression for $\Phi_j(z_j)$ which is

$$\Phi_j(z_j) = -g_j(s_1,s_2)\left\{\frac{Q\sqrt{c+d}}{\sqrt{z_j}(z_j+c+d)} - 2Y\sqrt{\frac{a}{z_j}} + iY\ell n\left(\frac{i\sqrt{z_j}+\sqrt{d}}{i\sqrt{z_j}-\sqrt{d}}\right)\right\} . \tag{73}$$

Thus, it follows that, for non-singular stresses at the tip of the plastic zone (the crack tip of the two superposed elastic solutions), the coefficient of $1/\sqrt{z_j}$ must be zero. Then, the following expression relating the ratio Q/Y to the geometric quantities must hold:

$$\frac{Q}{Yd} = 2\sqrt{(c+d)/d} . \tag{74}$$

The expressions for $\phi_j(z_j)$ are then

$$\phi_j(z_j) = Yg_j(s_1,s_2)\left\{2\sqrt{z_j d} - i(d+z_j)\ell n\left(\frac{i\sqrt{z_j}+\sqrt{d}}{i\sqrt{z_j}-\sqrt{d}}\right) + 2i\sqrt{d(c+d)}\ \ell n\left(\frac{i\sqrt{z_j}+\sqrt{c+d}}{i\sqrt{z_j}-\sqrt{c+d}}\right)\right\} . \tag{75}$$

This displacement, u_2^+, of the upper crack surface may be obtained by substitution of Equation (75) into Equation (62) with z_j equal to x_1. The result is

$$u_2^+ = \frac{s_1(s_2^2-1)Y}{\pi\mu[4s_1s_2-(1+s_2^2)^2]}\left\{2\sqrt{-(x_1d)} - (d+x_1)\ln\left(\frac{\sqrt{d}-\sqrt{-x_1}}{\sqrt{d}+\sqrt{-x_1}}\right)\right.$$

$$\left. + 2\sqrt{d(c+d)}\ln\left(\frac{\sqrt{c+d}-\sqrt{-x_1}}{\sqrt{c+d}+\sqrt{-x_1}}\right)\right\} \quad x<0 \ . \tag{76}$$

The length d of the plastic zone is independent of velocity and is related to Q/Y and the distance c of the load Q from the physical crack tip by Equation (74). The relationship is shown graphically in Figure 15.

Since the plastic zone length is independent of velocity a contour C which surrounds the plastic zone and is fixed in size with respect to time may be used in calculating the energy dissipation for this model. Then, the path independent integral around the contour of Equation (8) may be evaluated by shrinking C onto the boundary of the plastic zone. As a result, the expression for G_I is

$$G_I = -\int_L T_i \frac{\partial u_i}{\partial x_1}\, ds = \int_L \sigma_{22} \frac{\partial u_1}{\partial x_1}\, dx_1 \ . \tag{77}$$

In the case of perfect plasticity considered here, σ_{22} is equal to Y, the constant yield stress. Therefore

$$G_I = Y\int_L \frac{\partial u_2}{\partial x_1}\, dx_1 = Y[u_2]_L \tag{78}$$

or

$$G_I = Y\delta_T \tag{79}$$

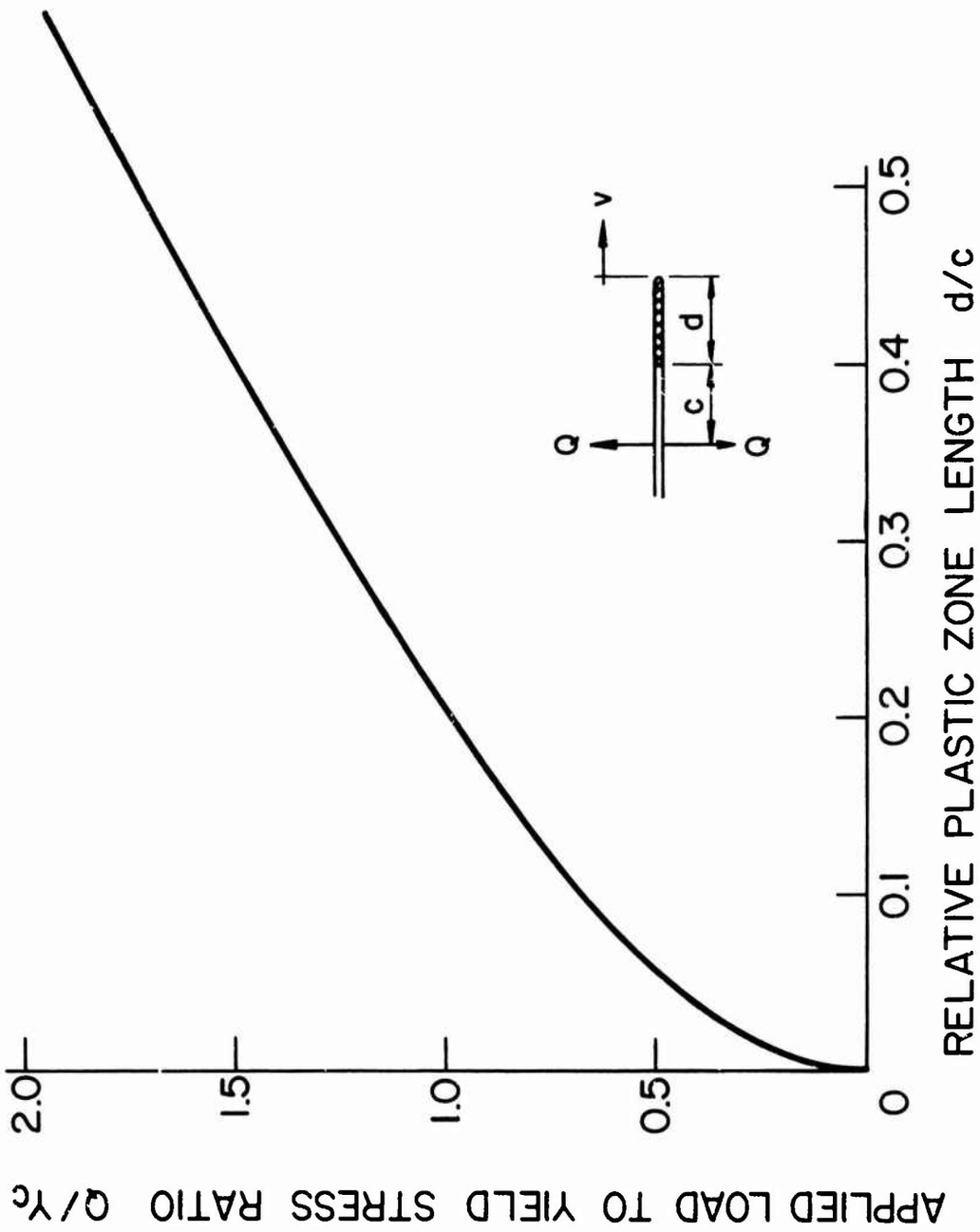

Figure 15. Finiteness Condition for Semi-Infinite Crack.

where δ_T is the crack opening displacement which is defined in terms of the displacements u_2^+ and u_2^- of the upper and lower crack surfaces at $x_1 = -d$ as

$$\delta_T = [u_2^+ - u_2^-]_{x_1 = -d} \quad . \tag{80}$$

Then making use of Equation (76), the expression for for the semi-infinite crack model is

$$\frac{\delta_T}{2} = \frac{2(s_2^2-1)Ys_1}{\pi\mu[4s_1s_2-(1+s_2^2)^2]} \left\{ d + \sqrt{d(c+d)}\ \ell n \left(\frac{\sqrt{c+d} - \sqrt{d}}{\sqrt{c+d} + \sqrt{d}} \right) \right\} \quad . \tag{81}$$

For convienience, using the above, the energy release rate may be written as the product of the normalized elastic value and a function of Q/YC. That

$$\frac{G_I}{G_I^*} = \frac{G_{I_{el}}}{G_I^*} f(q) \tag{82}$$

with q = Q/YC and

$$f(q) = \frac{2}{q^2} \left\{ 1 - \sqrt{1-q^2} + p\ell n(q + \sqrt{1+q^2}) \right\} \quad . \tag{83}$$

Figure 16 is a plot of f(q) versus q. Note that f(q) is equal to the ratio of G_I to the corresponding elastic value $G_{I_{el}}$, at a given crack speed.

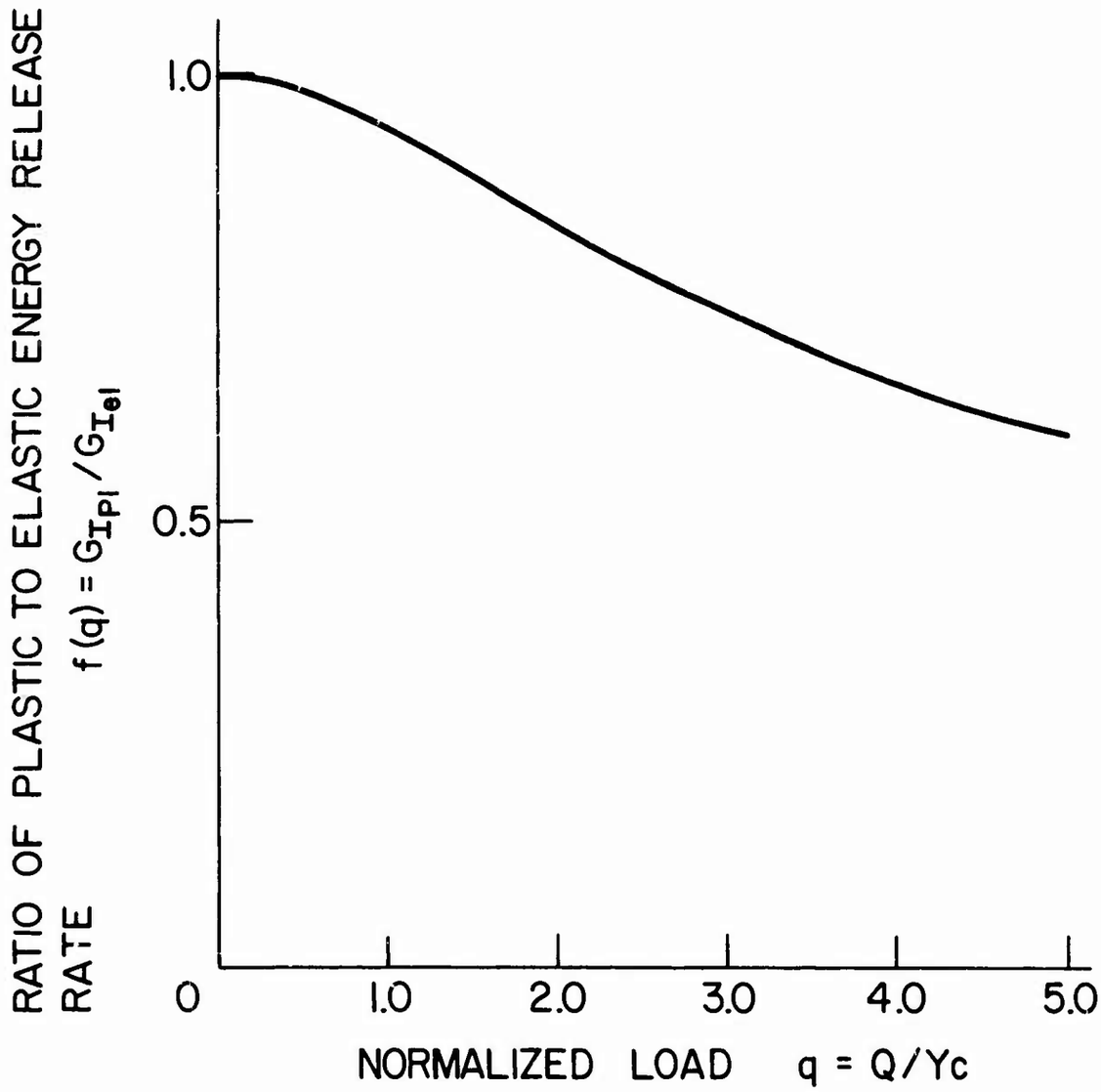

Figure 16. Ratio of Plastic to Elastic Energy Release Rate as a Function of Normalized Load for Semi-Infinite Crack.

4.4 CONSTANT LENGTH CRACK

Consider next the problem of a crack of fixed length 2c which propagates with a fixed velocity v. This crack model, with a Dugdale plastic zone is shown in Figure 17. With a=c, the elastic case would be depicted.

As for the semi-infinite crack model, the general results of Appendix I apply for the elastic results. Thus, Equation (64) also applies for the finite crack problem with G_I^* the static energy release rate now being

$$G_I^* = \frac{\pi P^2 c}{2\mu(1+\nu)} . \tag{84}$$

The analysis for the plastic case is similar to that used for the semi-infinite crack. Using the results of Sih [12] solutions for the sectionally holomorphic functions $\Phi_j(z_j)$, for a crack of length 2a, in an infinite elastic medium, when $\sigma_{12} = 0$ for all x on the crack line, are of the form

$$\Phi_j(z_j) = \frac{1}{2\pi i\sqrt{z_j^2-a^2}} \int_{-a}^{+a} \frac{f_j(\xi)\sqrt{\xi^2-a^2}}{\xi-z_j} d\xi + \frac{\Gamma_j}{\sqrt{z_j^2-a^2}} \tag{85}$$

where the functions f_1, f_2, Γ_1 and Γ_2 are

$$f_1(\xi) = \frac{(1+s_2^2)(\sigma_{22}^+ + \sigma_{22}^-)}{(1+s_2^2)^2 - 4s_1s_2} \tag{86}$$

$$f_2(\xi) = -\frac{4s_1s_2}{(1+s_2^2)} f_1(\xi) \tag{87}$$

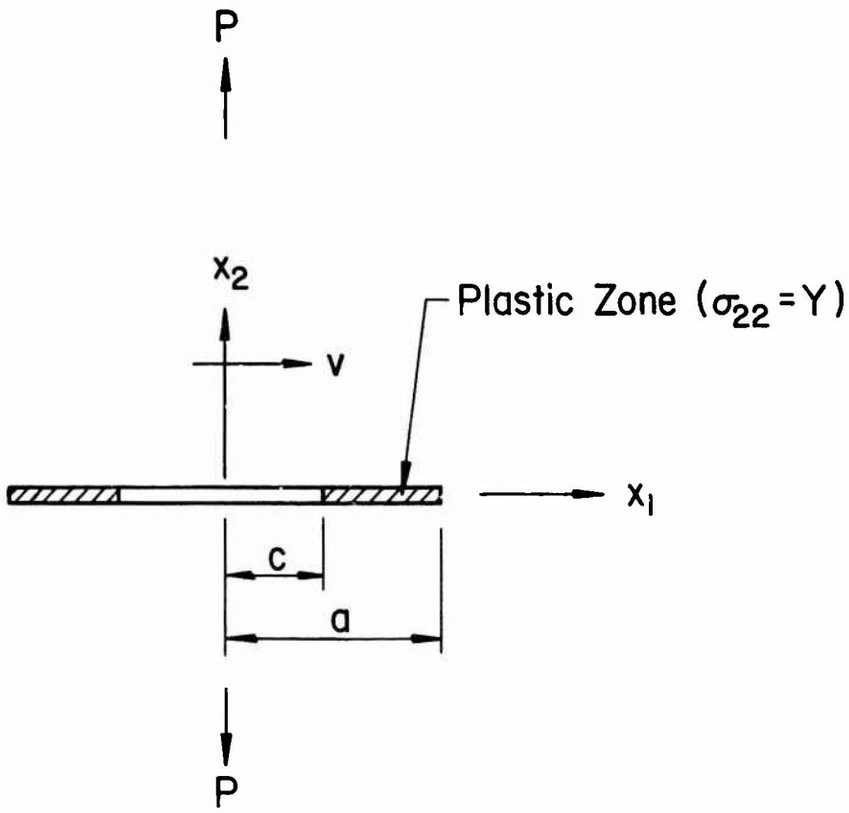

Figure 17. Constant Length Crack With Dugdale Plastic Zone Propagating with Velocity.

$$\Gamma_1 = -\frac{\sigma_{11}^{\infty} + \sigma_{22}^{\infty}}{2(s_1^2 - s_2^2)} \tag{88}$$

$$\Gamma_2 = \frac{\sigma_{22}^{\infty}}{1+s_2^2} + \frac{\sigma_{11}^{\infty} + \sigma_{22}^{\infty}}{2(s_1^2 - s_2^2)} \tag{89}$$

with σ_{22}^{+} and σ_{22}^{-} being normal stresses on the upper and lower sides of the crack and with σ_{11}^{∞} and σ_{22}^{∞} being the stresses at infinity.

Consider first the problem where concentrated loads Q are acting on the upper and lower crack surfaces at $x_1 = +b$, $-b$ (see Figure 18). For this case, $\Gamma_1 = \Gamma_2 = 0$ and

$$f_1(\xi) = -\frac{2(1+s_2^2)P}{(1+s_2^2)^2 - 4s_1 s_2}\,[\delta(\xi+b) + \delta(\xi-b)]. \tag{90}$$

Then $\Phi_j(z_j)$ are

$$\Phi_j(z_j) = -2g_j(s_1,s_2)Q\,\frac{\sqrt{a^2-b^2}\;z_j}{(z_j^2-b^2)\sqrt{z_j^2-a^2}} \tag{91}$$

where $g_j(s_1,s_2)$ are given by Equations (67) and (68).

The above expression may be used to generate the solution to problems where uniform tractions are imposed upon the crack edge. For the case shown in Figure 19 where the portions of the crack surface extending from $|x_1| = c$ to $|x_1| = a$ are under pressure p, the functions $\Phi_j(z_j)$ may be obtained by letting $Q = pd\xi$ and $b = \xi$ and integrating

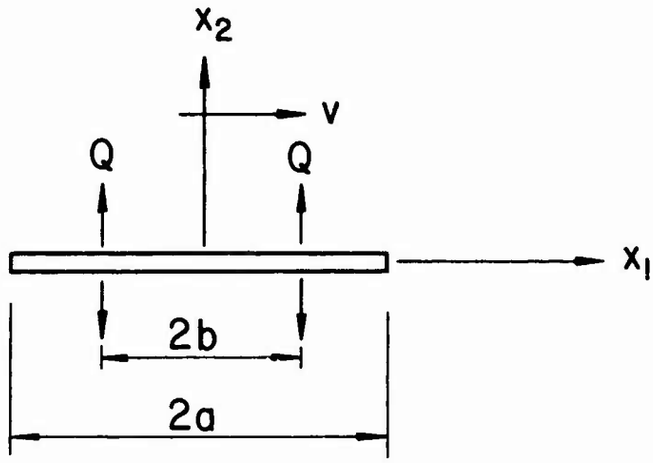

Figure 18. Constant Length Crack Propagating with Velocity v and Loaded by Concentrated Forces.

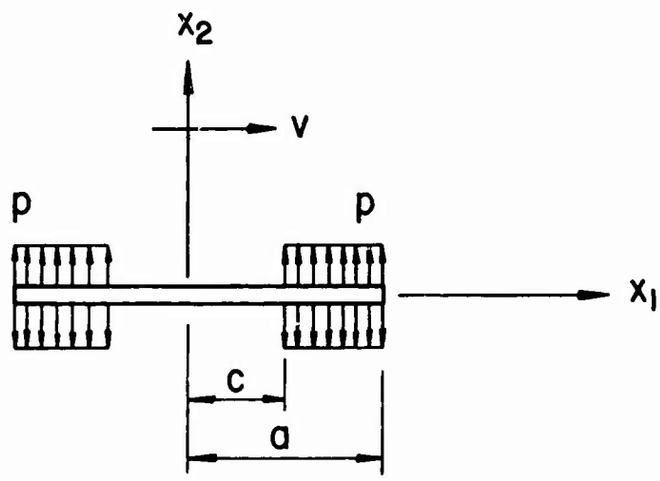

Figure 19. Constant Length Crack Propagating with Velocity v and Loaded Uniformly over Portion of Crack Surface.

Equation (91) over the range $c \leq \xi \leq a$. The result of this operation is

$$\Phi_j(z_j) = -g_j(s_1,s_2)p \left\{ 2z_j \cos^{-1}(c/a) - i \log\left(\frac{z_j\sqrt{a^2-c^2} - c\sqrt{a^2-z_j^2}}{z_j\sqrt{a^2-c^2} + c\sqrt{a^2-z_j^2}} \right) + \pi \right\} . \tag{92}$$

In order to obtain the solution for a crack length 2c with a plastic zone of length (a-c), the above solution with $p = -Y$ is added to the elastic solution of a crack of length 2a under uniform tensile stress P at infinity (see Figure 17). The latter solution, which may be obtained from Equations (85) through (89)[12] is

$$\Phi_j(z_j) = g_j(s_1,s_2)P\pi \left[\frac{z_j}{\sqrt{z_j^2-a^2}} - 1 \right] + A_j \tag{93}$$

with

$$A_1 = - \frac{P}{2(s_1^2-s_2^2)} \tag{94}$$

$$A_2 = \frac{P}{1+s_2^2} + \frac{P}{2(s_1^2-s_2^2)} . \tag{95}$$

Inspection of $\Phi_j(z_j)$ for the two cases reveals that, for the superposition of the two solutions to satisfy the Dugdale hypothesis of finite stress in the neighborhood of $|x_1| = a$, the following condition must be met:

$$\frac{c}{a} = \cos\left[\frac{P}{Y}\frac{\pi}{2}\right] . \tag{96}$$

The superposed solution that satisfies this condition is then

$$\Phi_j(z_j) = -g_j(s_1,s_2)Y\left\{ i \log\left(\frac{z_j\sqrt{a^2-c^2} - c\sqrt{a^2-z_j^2}}{z_j\sqrt{a^2-c^2} + c\sqrt{a^2-z_j^2}}\right) -\pi\left(1 + \frac{P}{Y}\right)\right\} + A_j . \tag{97}$$

In order to evaluate displacements, the functions $\phi_j(z_j)$ are obtained by integrating the preceding expression with respect to z_j. Thus,

$$\phi_j(z_j) = -g_j(s_1,s_2)Y\left\{ iz_j\log\left(\frac{z_j\sqrt{a^2-c^2} - c\sqrt{a^2-z_j^2}}{z_j\sqrt{a^2-c^2} + c\sqrt{a^2-z_j^2}}\right) - ib\log\left(\frac{\sqrt{a^2-c^2} - \sqrt{a^2-z_j^2}}{\sqrt{a^2-c^2} + \sqrt{a^2-z_j^2}}\right) -\pi\left(1+\frac{P}{Y}\right)z_j\right\} + A_j z_j . \tag{98}$$

Then, by Equation (62) the displacement on the upper portion of the crack surface is

$$u_2^+ = \frac{s_1(1-s_2^2)Y}{\pi\mu[4s_1s_2-(1+s_2^2)^2]}\left\{x_1\log\left|\frac{x_1\sqrt{a^2-c^2} - c\sqrt{a^2-x_1^2}}{x_1\sqrt{a^2-c^2} + c\sqrt{a^2-x_1^2}}\right| + c\log\left|\frac{\sqrt{a^2-c^2} + \sqrt{a^2-x_1^2}}{\sqrt{a^2-c^2} - \sqrt{a^2-x_1^2}}\right|\right\} \quad |x|\leq a . \tag{99}$$

The crack opening displacement, δ_T, at $|x_1| = c$ is

$$\delta_T = \frac{4s_1(1-s_2^2)Yc}{\pi\mu[4s_1s_2-(1+s_2^2)^2]} \log(a/c) \tag{100}$$

or, making use of Equation (96)

$$\delta_T = \frac{4s_1(1-s_2^2)Yc}{\pi\mu[4s_1s_2-(1+s_2^2)^2]} \log[\sec(\frac{\pi P}{2Y})] \ . \tag{101}$$

Use of the Dugdale hypothesis has led to a relationship between the length a of the plastic zone plus the crack, the length c of the crack, the applied stress P, and the yield stress Y. The relationship is again independent of crack speed and, since Equation (96) is the same as Equation (56), is identical to the static result. Thus, calculating the energy release rate the same reasoning as was used for the case of the semi-infinite crack applies and the general expressions of Equations (77) - (79) and Equation (82) are valid in this case also, with f(q) being given as,

$$f(q) = \frac{8}{\pi^2 q^2} \log(\sec[\frac{\pi}{2} q]) \tag{102}$$

where

$$q = P/Y \ . \tag{103}$$

Again, it should be noted that f(q) in Equation (102) is equal to the ratio of the plastic energy dissipation to the elastic energy release rate for the Yoffé model. This ratio,

independent of crack speed, is plotted in Figure 21. Thus, for a given value of P/Y the value of $G_{I_{pl}}/G_I^*$ may be obtained by multiplying the plot in Figure 20 by the corresponding value of f(q) obtained from Figure 21.

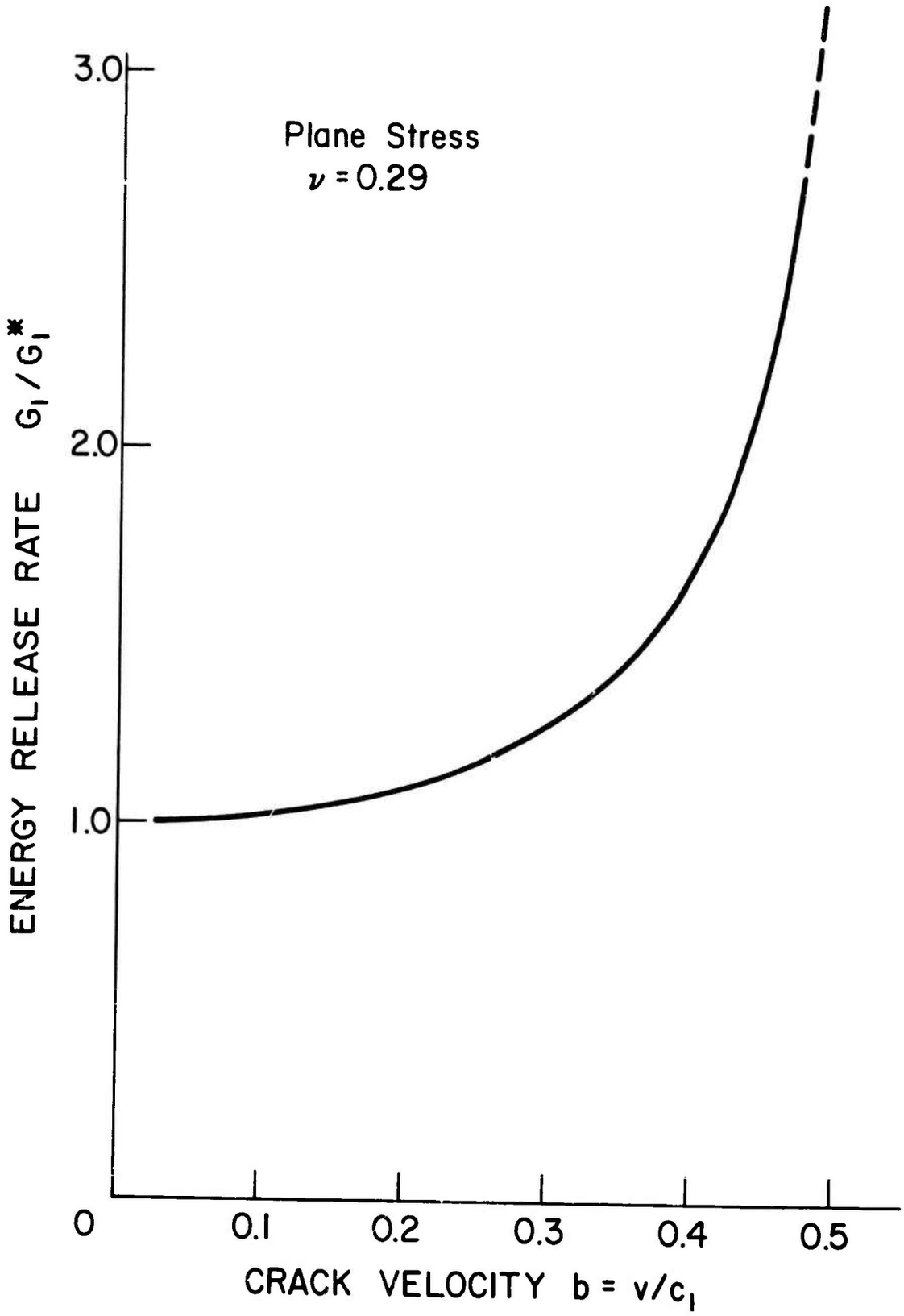

Figure 20. Energy Release Rate Versus Crack Speed for Fixed Length and Semi-Infinite Dynamic Crack Models.

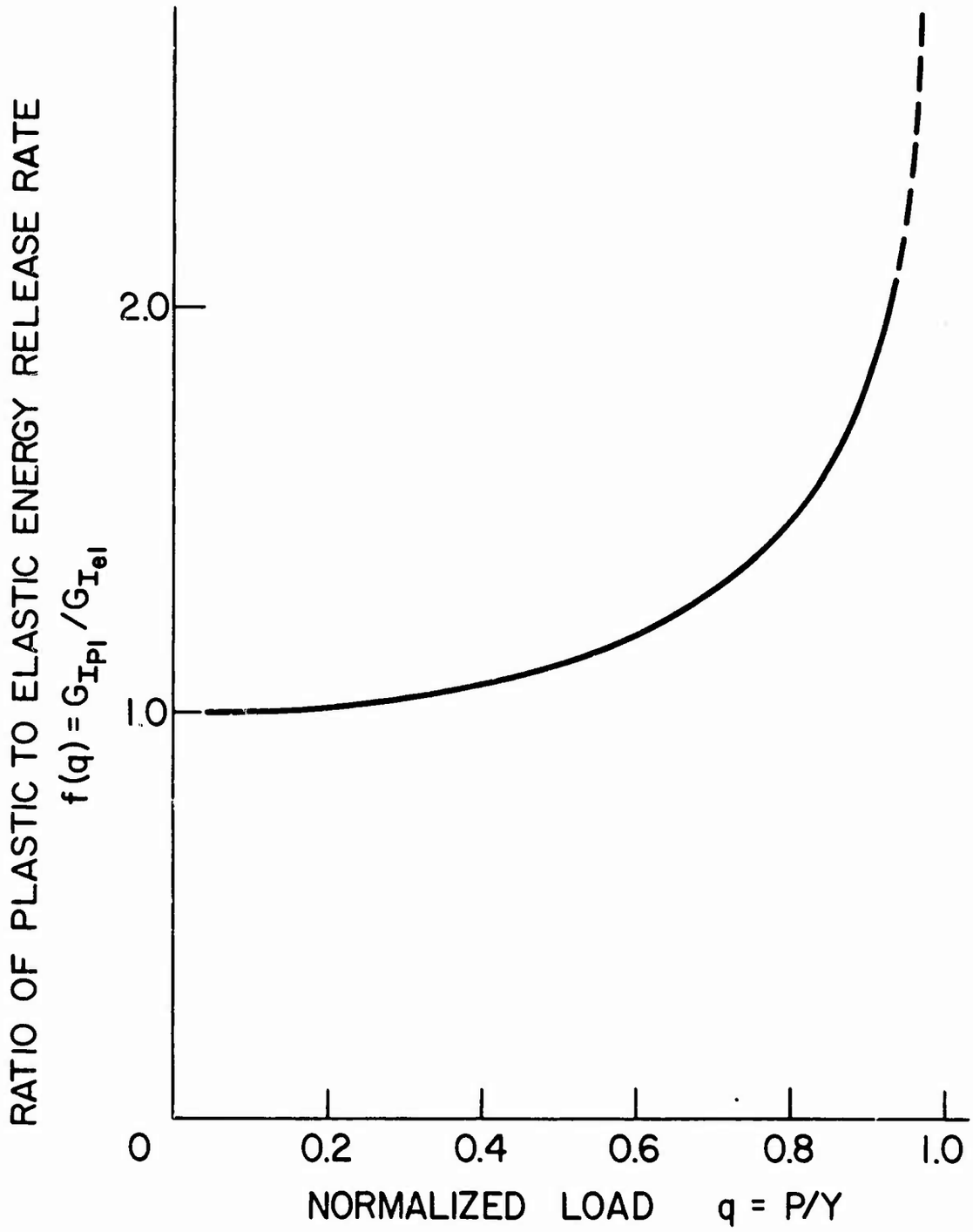

Figure 21. Ratio of Plastic to Elastic Energy Release Rate as a Function of Normalized Load for Fixed Length Crack.

SECTION V

PLASTIC FLOW AROUND AN EXPANDING CRACK

A more realistic crack model for the projectile penetration problem should involve a central crack in the target material moving at both ends. As before, the material along the lines of expected crack extension will be assumed to flow plastically and to move with the crack but at a different velocity. The energy released as a function of the crack speed will be examined.

5.1 CRACK EXPANDING ELASTICALLY

Broberg [11] considered the case of an infinite elastic plate, under uniform tensile stress P, with a crack opening from zero length and extending with uniform velocity v. The stresses and displacements near the crack tip for this case are given in Appendix I. It should be noted that this model would apply to the case where an expanding crack has reached a length several times greater than its original length prior to propagation (after the initial acceleration stage).

One of the important contributions of the Broberg solution was that it allowed a more realistic estimate of the rate at which energy is dissipated at the crack tip, i.e., the energy release rate G_I. Using Equations (14) and (I-11), a plot of the normalized energy release rate, G_I/G_I^*, versus the ratio of crack speed to dilatational wave velocity is

given for steel (ν =0.29) in Figure 26. Two factors should be kept in mind when using this plot. First, the normalization with respect to G_I^* implies that the value of G_I at a given velocity is directly proportional to the instantaneous crack length c, since, with the value $k_I = P\sqrt{c}$,

$$G_I = \left(\frac{G_I}{G_I^*}\right) G_I^* = \left(\frac{G_I}{G_I^*}\right) \frac{\pi(\kappa+1)}{8\pi} P\ c\ .$$

Secondly, the value determined is the predicted amount of elastic energy irreversibly absorbed by the crack tip at a given velocity; the mechanism by which this energy is absorbed is not specified. Thus, in order to derive a functional relationship between the material parameters, crack length, load, and velocity, this mechanism must be properly modeled.

If, for example, the Griffith criterion of direct conversion into surface energy is used, the velocity could be approximated through the relation

$$G_I = 2\gamma$$

or

$$\frac{G_I}{G_I^*} = \frac{16\gamma\mu}{\pi(\kappa+1)P^2c}$$

where γ is the specific surface energy. Thus, the predicted limiting velocity as $c \to \infty$ would be the Rayleigh wave velocity c_R. However, the above criterion can only be applied to an

exceedingly brittle material such as glass, with the assumption that γ is independent of crack speed. Experimental evidence supports the fact that crack velocities in ductile materials are dependent upon a dissipative process and may be limited to speeds which are only a fraction of c_R [29].

5.2 PLASTIC YIELDING AROUND THE CRACK

Incorporation of the Dugdale hypothesis into the material of dynamic crack propagation allows consideration of plastic energy dissipation. However, as will be seen, this does not satisfactorily specify the absorption mechanism. That is, again an additional condition dealing with material behavior is necessary if one desires the limiting velocity for a given material and applied stress. The information that is obtained here is the amount of energy dissipated by a very specialized plastic zone for a given crack velocity.

The formulation of the elastic boundary value problem that is equivalent to the elastic-plastic problem of a uniformly expanding crack with a Dugdale plastic zone ahead of the crack tip is made in the same fashion as for the steady-state and static problems. Atkinson [14] considered this problem for a crack whose tips have a velocity v with a plastic zone, the end of which is traveling at velocity β. The equivalent elastic problem, then, consists of an infinite plate under uniform tensile stress P with a crack of length $2a = 2\beta t$ upon which tensile stress Y is applied over the region $vt \leq |x_1| \leq \beta t$. The expressions for

normal stress σ_{22}, ahead of the plastic zone and for the second derivative with respect to time of the displacement, u_2, of the crack surface are

$$\sigma_{22} = -\frac{B}{2}\left[\int_r^1 \frac{(s-2k^2)^2 ds}{s\sqrt{s(1-s)s-\beta_0^2)^3}} - 4k^3 \int_r^{k^2} \frac{\sqrt{k^2-s}}{s\sqrt{s(s-\beta_0^2)^3}}\, ds\right]$$

$$+ \frac{TA}{2}\left[\int_r^1 \frac{(s-2k^2)^2 ds}{s(s-b^2)\sqrt{s(1-s)(s-\beta_0^2)^3}}\right.$$

$$\left. - 4k^3 \int_r^{k^2} \frac{\sqrt{k^2-s}\, ds}{s(s-b^2)\sqrt{s(s-\beta_0^2)^3}}\right] + P \qquad (104)$$

for $x_2 = 0$ and $|x_1| > \beta_0\tau \left(\text{or } r > \beta_0^2\right)$ and

$$\frac{\partial^2 u_2}{\partial \tau^2} = \frac{-\mathrm{Re}[F(r)]}{2\pi k^4 \rho c_1^2 |x_1|}\left\{\frac{(P-Y)\beta_0 r}{r-\beta_0^2} + \frac{Ybr}{r-b^2} + \frac{1}{2}\int_{\beta_0^2}^1 \left[\frac{r}{r-s}\right.\right.$$

$$\left.\left. - \frac{\beta_0 r}{\sqrt{s}(r-\beta_0^2)}\right] \phi(s)ds\right\} \quad 0<r<\beta_0^2 \quad \text{or } 0<|x_1|<\beta_0\tau \qquad (105)$$

where

$$\tau = c_1 t \qquad k = c_2/c_1$$

$$b = v/c_1 \qquad r = x_1^2/\tau^2 \qquad (106)$$

$$\beta_0 = \beta/c_1$$

and Y is the yield stress of the material. The elastic wave velocities, c_1 and c_2, are described in Appendix I. The functions F(r) and $\phi(r)$ are

$$F(r) = \frac{4k^4 r^{32}\sqrt{1-r}}{(r-2k^2)^2-4k^3\sqrt{(1-r)(k^2-r)}} \tag{107}$$

and

$$\phi(r) = \begin{cases} [B - \frac{TA}{r-b^2}] \frac{(r-2k^2)^2-4k^3\sqrt{(1-r)(k^2-r)}}{r\sqrt{(1-r)(r-\beta_0^2)^3}}, & \text{for } \beta_0^2<r<k^2 \\ [B - \frac{TA}{r-b^2}] \frac{(r-2k^2)^2}{r\sqrt{(1-r)(r-\beta_0^2)^3}} & k^2<r<1 \end{cases} \tag{108}$$

where

$$TA = \frac{2Yb^3\sqrt{(1-b^2)(\beta_0^2-b^2)^3}}{\pi[4k^3\sqrt{(1-b^2)(k^2-b^2)}-(b^2-2k^2)^2]} \tag{109}$$

and where the following equation may be used to obtain B,

$$B = \frac{2(P-Y)\beta_0}{\pi} + \frac{2Yb}{\pi} + \frac{1}{\pi}\int_{\beta_0^2}^{1} \frac{\sqrt{s}-\beta_0}{\sqrt{s}}\,\phi(s)ds\ . \tag{110}$$

An algebraic expression for B in terms of elliptic integrals may be obtained by combination of Equations (108), (109), and (110). The result obtained by Atkinson has been corrected here and is as follows

$$BZ_1 = 2(P-Y)\beta_0 - \frac{TA}{b^2} Z_2 \tag{111}$$

where

$$Z_1 = \frac{2[\beta_0^2-4k^2\beta_0^2 +4k^2]}{\beta_0(1-\beta_0^2)} K(\sqrt{1-\beta_0^2}) +$$

$$- \frac{2[\beta_0^4-4k^2(1+k^2)\beta_0^2+8k^4]}{\beta_0^3(1-\beta_0^2)} E(\sqrt{1-\beta^2})$$

$$- \frac{8k^2}{\beta_0} K(\sqrt{1-\beta_0^2/k^2}) + \frac{16k^4}{\beta_0^3} E(\sqrt{1-\beta_0^2/k^2}) \qquad (112)$$

and

$$Z_2 = - \frac{2b^2(\beta_0^2-2k^2)^2}{\beta_0(\beta_0^2-b^2)(1-\beta_0^2)} K(\sqrt{1-\beta_0^2})$$

$$+ \frac{2b^2(\beta_0^2-2k^2)^2-8k^4(\beta_0^2-b^2)(1-\beta_0^2)}{\beta_0^3(\beta_0^2-b^2)(1-\beta_0^2)} E(\sqrt{1-\beta_0^2})$$

$$+ \frac{8k^2b^2}{\beta_0(\beta_0^2-b^2)} K(\sqrt{1-\beta_0^2/k^2}) + \frac{8k^4(\beta_0^2-2b^2)}{\beta^3(\beta_0^2-b^2)} E(\sqrt{1-\beta_0^2/k^2})$$

$$+ \frac{2\beta_0(b^2-2k^2)^2}{(1-b^2)(\beta_0^2-b^2)} \Pi\left(\frac{1-\beta_0^2}{1-b^2}, \sqrt{1-\beta_0^2}\right)$$

$$- \frac{8k^2\beta_0}{(\beta_0^2-b^2)} \Pi\left(\frac{1-\beta_0^2/k^2}{1-b^2/k^2}, \sqrt{1-\beta_0^2/k^2}\right). \qquad (113)$$

The functions K, E, and Π, are complete elliptic integrals of the first, second, and third kinds, respectively, and are defined in Byrd and Friedman [33].

Equation (105) must be integrated twice in order to obtain the displacement of the crack line. To this end, Equation (105) is rewritten as

$$\frac{\partial^2 u_2}{\partial \tau^2} = - \frac{r\mathrm{Re}[F(r)]}{2\pi k^4 \rho c_1^2 |x_1| (r-\beta_0^2)} \left\{ (P-Y)\beta_0 + \frac{(r-\beta_0^2)}{(r-b^2)} Yb - \right.$$

$$- \frac{1}{2} \int_{\beta_0^2}^{1} \frac{(s-\beta_0^2)}{(s-r)} \phi(s)ds + \frac{1}{2} \int_{\beta_0^2}^{1} \frac{\sqrt{s}-\beta_0}{\sqrt{s}} \phi(s)ds \Bigg\} \quad 0<r<\beta_0^2 \ . \tag{114}$$

Application of Equation (110) simplifies the preceding equation to read

$$\frac{\partial^2 u_2}{\partial \tau^2} = - \frac{rRe[F(r)]}{2\pi k^4 \rho c_1^2 |x_1| (r-\beta_0^2)} \left\{ \frac{\pi}{2} B + \frac{(b^2-\beta_0^2)Yb}{r-b^2} \right.$$

$$\left. - \frac{1}{2} \int_{\beta_0^2}^{1} \frac{(s-\beta_0^2)}{(s-r)} \phi(s)ds \right\} \quad 0<r<\beta_0^2 \ . \tag{115}$$

Recalling that the expression for $\phi(s)$ is given in Equation (108), the integral in Equation (115) may be broken down into four integrals which may be evaluated by well known methods of complex variable theory [30]. After further simplification through Equations (107) and (109), the resulting expression for $\partial^2 u_2/\partial\tau^2$ is

$$\frac{\partial^2 u_2}{\partial \tau^2} = - \frac{r}{\rho c_1^2 |x_1| (\beta_0^2-r)} \left\{ \frac{Br^{\frac{1}{2}}}{\sqrt{\beta_0^2-r}} - \frac{TAr^{\frac{1}{2}}}{(r-b^2)\sqrt{\beta_0^2-r}} \right\}. \tag{116}$$

$$0<r<\beta_0^2$$

For any function $g(r,x)$, where r is given in Equation (106), the chain rule of elementary calculus allows the derivative with respect to τ of g to be written

$$\frac{\partial g}{\partial \tau} = \frac{\partial g}{\partial r} \frac{\partial r}{\partial \tau} = -2 \frac{r^{3/2}}{|x_1|} \frac{\partial g}{\partial r} \ . \tag{117}$$

Thus, Equation (116) may be written

$$\frac{\partial}{\partial r}\left(\frac{\partial u_2}{\partial \tau}\right) = \frac{1}{2\rho c_1^2}\left\{\frac{B}{(\beta_0^2-r)^{3/2}} - \frac{TA}{(r-b^2)(\beta_0^2-b^2)^{3/2}}\right\} . \tag{118}$$

Integration of the above expression yields

$$\frac{\partial u_2}{\partial \tau} = \frac{1}{2\rho c_1^2}\left\{\frac{B}{(\beta_0^2-r)^{1/2}} - \frac{2TA}{(\beta_0^2-b^2)(\beta_0^2-r)^{1/2}}\right. \tag{119}$$

$$\left. - \frac{TA}{(\beta_0^2-b^2)^{3/2}} \log\left|\frac{\sqrt{\beta_0^2-b^2} - \sqrt{\beta_0^2-r}}{\sqrt{\beta_0^2-r} + \sqrt{\beta_0^2-b^2}}\right|\right\} \quad 0<r<\beta_0^2 .$$

Again making use of Equation (117), a second integration with respect to r leads to the result

$$u_2 = \frac{|x_1|}{2\rho c_1^2}\left\{\frac{2B}{\beta_0^2 r^{\frac{1}{2}}}\sqrt{\beta_0^2-r} - \frac{2TA\sqrt{\beta_0^2-r}}{\beta_0^2(\beta_0^2-b^2)r^{\frac{1}{2}}}\right.$$

$$- \frac{TA}{(\beta_0^2-b^2)^{3/2}}\left[\frac{1}{r^{\frac{1}{2}}}\log\left|\frac{\sqrt{\beta_0^2-b^2} - \sqrt{\beta_0^2-r}}{\sqrt{\beta_0^2-r} + \sqrt{\beta_0^2-b^2}}\right|\right. \tag{120}$$

$$\left.\left. + \frac{1}{b}\log\left|\frac{r^{\frac{1}{2}}\sqrt{\beta_0^2-b^2} + b\sqrt{\beta_0^2-r}}{r^{\frac{1}{2}}\sqrt{\beta_0^2-b^2} - b\sqrt{\beta_0^2-r}}\right|\right]\right\} \quad 0<r<\beta_0^2 .$$

The condition that stress be bounded in the neighborhood of the points $|x_1|=\beta_0\tau$ is satisfied if the slope of the displacement of the crack surface is zero at $|x_1|=\beta_0\tau$. Differentiation of Equation (120) with respect to x_1 reveals that this condition requires that

$$B = \frac{TA}{\beta_0^2 - b^2} . \tag{121}$$

With elimination of B by the above relation, the expression for u_2 may be written in terms of x_1 and τ as

$$u_2 = - \frac{TA}{2\rho c_1^2 (\beta_0^2 - b^2)^{32} b} \left\{ \tau b \log \left| \frac{\tau\sqrt{\beta_0^2 - b^2} - \sqrt{\tau^2 \beta_0^2 - x_1^2}}{\sqrt{\tau^2 \beta_0^2 - x_1^2} + \tau\sqrt{\beta_0^2 - b^2}} \right| \right.$$

$$\left. + x_1 \log \left| \frac{x_1\sqrt{\beta_0^2 - b^2} + b\sqrt{\beta_0^2 \tau^2 - x_1^2}}{x_1\sqrt{\beta_0^2 - b^2} - b\sqrt{\beta_0^2 \tau^2 - x_1^2}} \right| \right\} . \tag{122}$$

5.3 FINITENESS CONDITION

Although Equation (122) does not explicity depend on the applied load P, there is implicit dependence through the relationship between B and TA of Equation (121). This equation together with Equations (111) through (113) imposes a functional dependence between the parameters P/Y, β_0, and b. Thus, in evaluating u, only two of these may be independently specified. Upon combination of Equations (111) through (113) with Equation (121), the finiteness condition may be represented by the equation

$$1 - P/Y = \frac{AT}{Y} \left\{ - \frac{1}{(\beta_0^2 - b^2)} K(\sqrt{1-\beta_0^2}) + \frac{4k^4}{b^2 \beta_0^2 (\beta_0^2 - b^2)} E(\sqrt{1-\beta_0^2}) \right.$$

$$- \frac{4k^4}{b^2 \beta_0^2 (\beta_0^2 - b^2)} E(\sqrt{1-\beta_0^2/k^2}) +$$

$$+ \frac{4k^2}{b^2(\beta_0^2-b^2)} \Pi\left(\frac{1-\beta_0^2/k^2}{1-b^2/k^2}, \sqrt{1-\beta_0^2/k^2}\right)$$

$$- \frac{(b^2-2k^2)^2}{b^2(1-b^2)(\beta_0^2-b^2)} \Pi\left(\frac{1-\beta_0^2}{1-b^2}, \sqrt{1-\beta_0^2}\right)\Bigg\} . \qquad (123)$$

Using the preceding equation, P/Y has been plotted as a function of relative plastic zone size $(\beta_0-b)/\beta_0$ for fixed values of β_0 in Figure 22 and for fixed values of b in Figure 23. The curve for β_0 =b=0 represents both the static case and the constant velocity fixed length crack. An important effect to be noted here is that, for a given value of P/Y, an increase in crack velocity causes a decrease in relative plastic zone size. Figure 24 shows the variation of β_0, the normalized velocity of the plastic zone tip, with the stress ratio P/Y when b is held fixed. It can be seen here that β_0 has a lower limit equal to the normalized crack speed b and reaches a maximum which is less than or equal to the normalized Rayleigh wave volocity when P/Y=1. The plastic zone tip reaches the Rayleigh wave speed only when the crack tip reaches the same speed.

5.4 ENERGY RELEASE RATE

For this model, the rate at which energy is dissipated by the moving crack tip is evaluated by the result of Equation (20) in Section II.

Making use of the relation

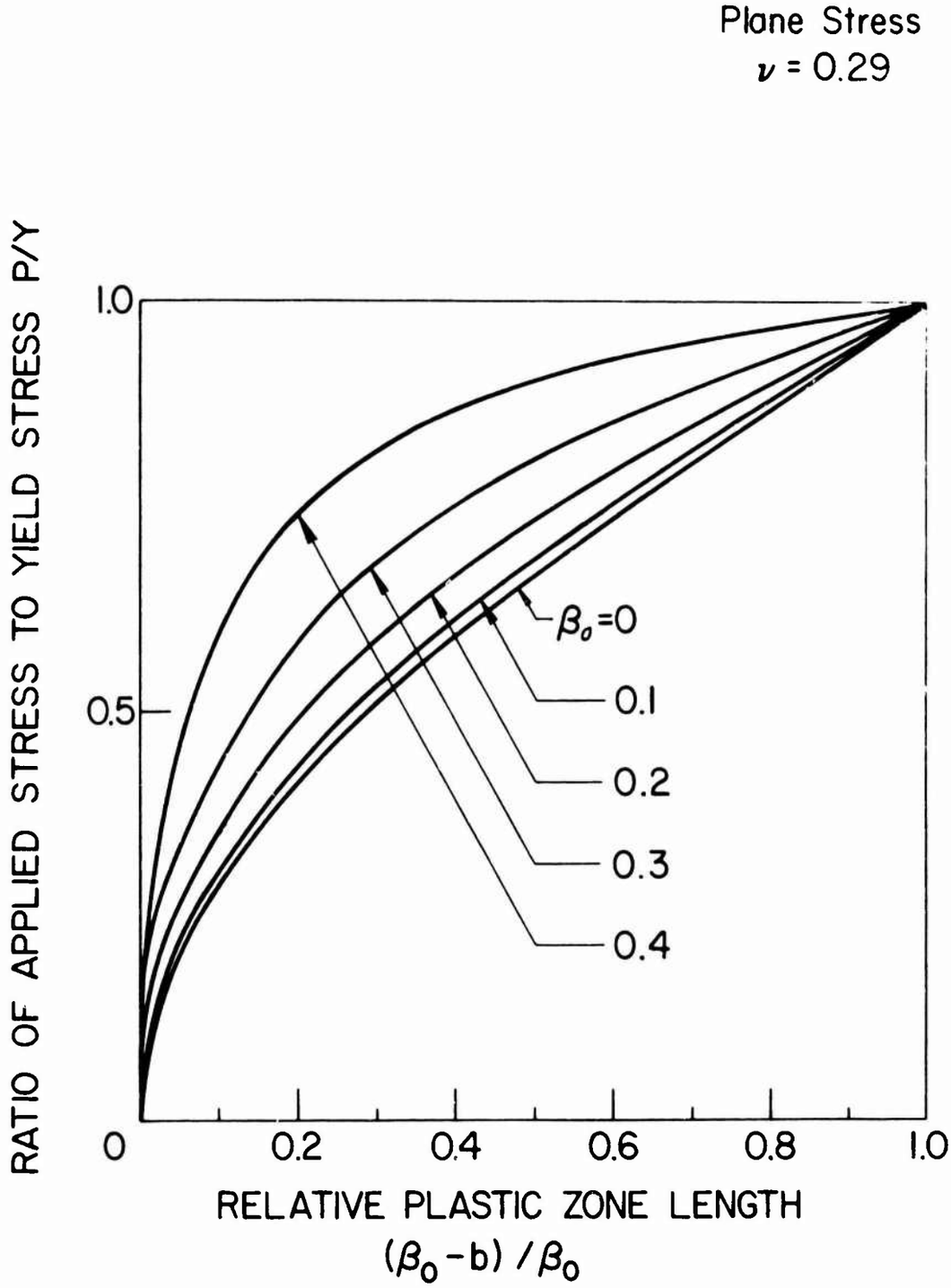

Figure 22. Finiteness Condition for Uniformly Expanding Crack. Plot of Ratio of Applied to Yield Stress versus Relative Plastic Zone Length for Various Velocities of the Tip of the Plastic Strip.

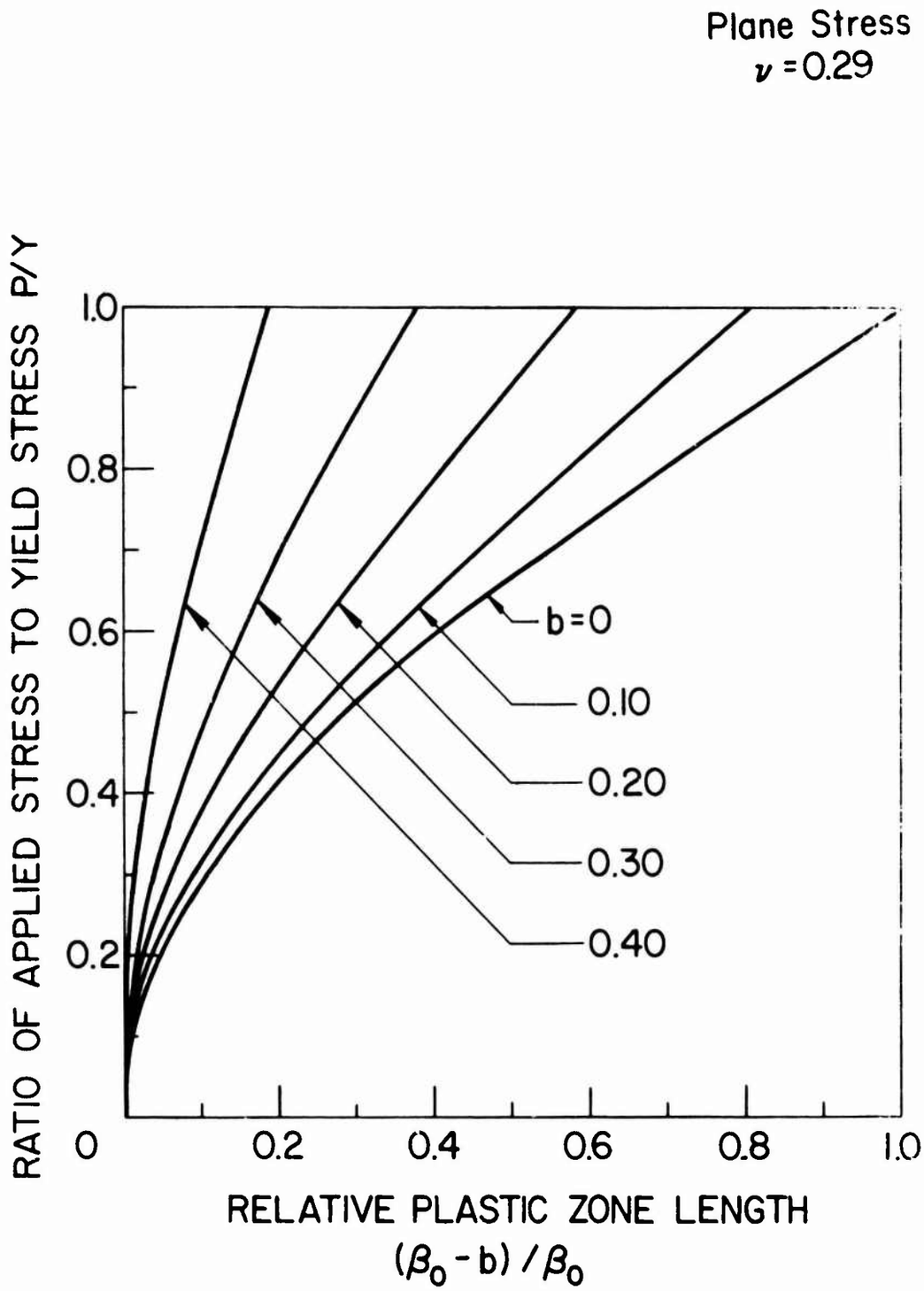

Figure 23. Finiteness Condition for Uniformly Expanding Crack. Plot of Ratio of Applied to Yield Stress versus Relative Plastic Zone Length for Various Crack Tip Velocities.

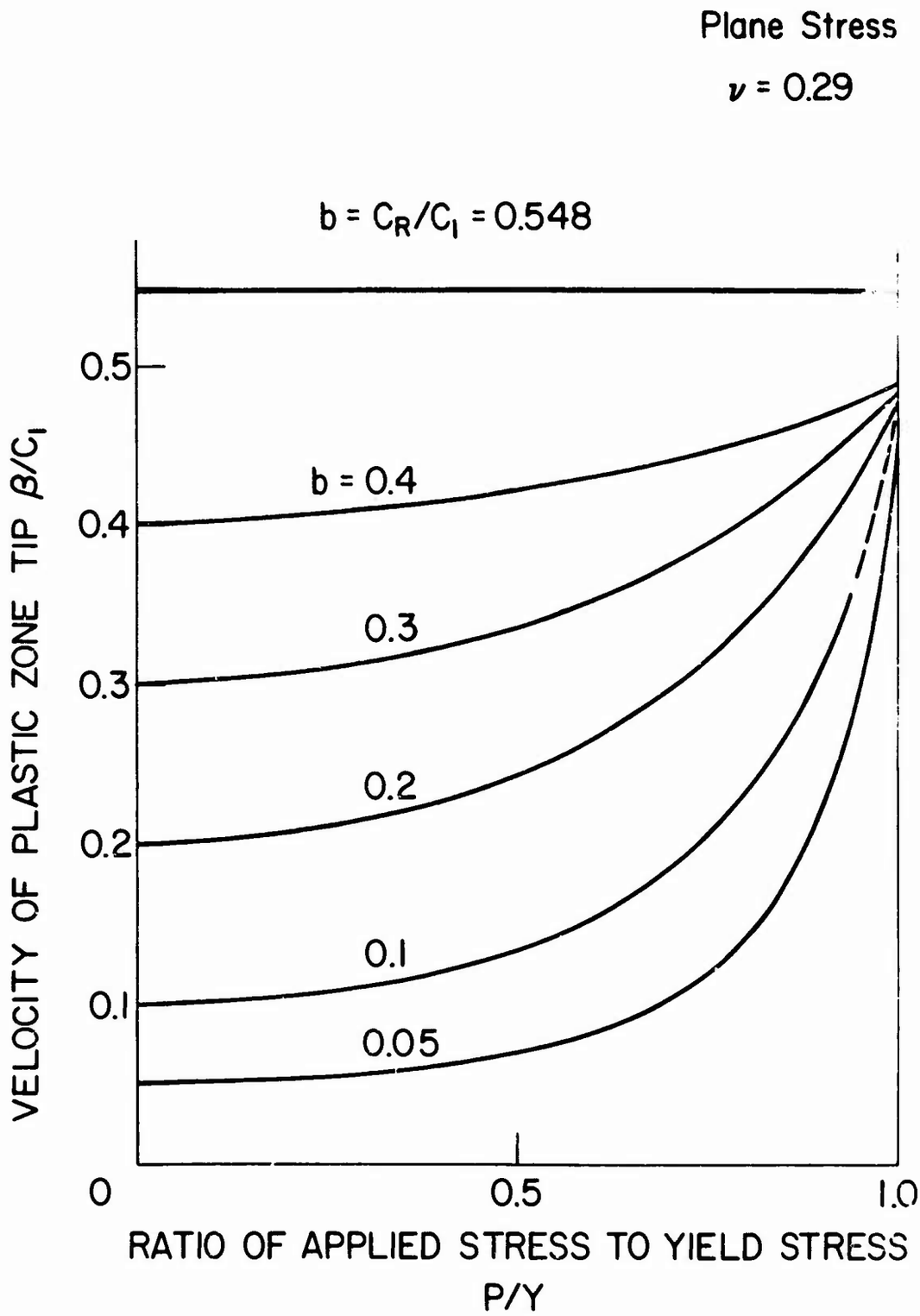

Figure 24. Finiteness Condition for Uniformly Expanding Crack. Plot of Normalized Velocity of Plastic Zone Tip versus Ratio of Applied to Yield Stress for Various Crack Tip Velocities.

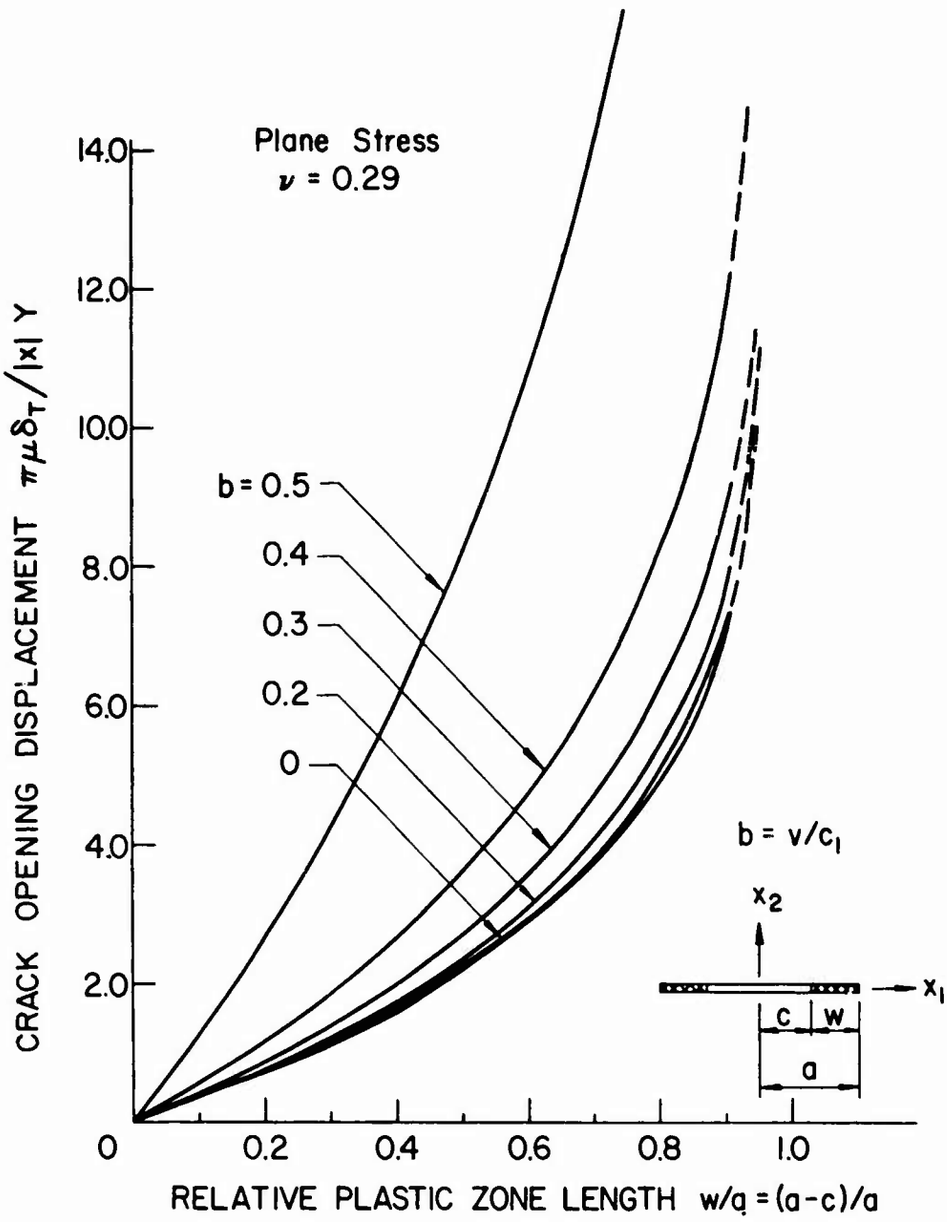

Figure 25. Plot of Normalized Crack Opening Displacement Versus Relative Plastic Zone Length for Various Crack Tip Velocities. Valid for Constant Length Crack and Uniformly Expanding Model.

$$\frac{\partial}{\partial\tau}\int_{b\tau}^{\beta_0\tau} u_2(x_1,\tau)dx_1 = \int_{b\tau}^{\beta_0\tau} \frac{\partial u_2}{\partial\tau}\, dx_1 + u_2(\beta_0\tau,\tau)\beta_0 - u_2(b\tau,\tau)b \tag{124}$$

and noting that $u_2(\beta_0\tau,\tau) = 0$, Equation (20) may be written as

$$G_I b = 2Yu_2(b\tau,\tau)b + 2Y\frac{\partial}{\partial\tau}\int_{b\tau}^{\beta_0\tau} u_2(x_1,\tau)dx_1 \,. \tag{125}$$

Upon substitution of Equation (122), the integral in the above equation may be expressed in the form

$$\int_{b\tau}^{\beta_0\tau} u_2(x_1,\tau)dx_1 = -\frac{TA}{2\rho c_1^2(\beta_0^2-b^2)^{3/2}b}(I_1 + I_2) \tag{126}$$

where

$$I_1 = \int_{b\tau}^{\beta_0\tau} \tau b\log\left[\frac{\tau\sqrt{\beta_0^2-b^2} - \sqrt{\tau^2\beta_0^2-x_1^2}}{\sqrt{\tau^2\beta_0^2-x_1^2} + \tau\sqrt{\beta_0^2-b^2}}\right] dx_1 \tag{127}$$

and

$$I_2 = \int_{b\tau}^{\beta_0\tau} x_1\log\left[\frac{x_1\sqrt{\beta_0^2-b^2} + b\sqrt{\beta_0^2\tau^2-x^2}}{x_1\sqrt{\beta_0^2-b^2} - b\sqrt{\beta_0^2\tau^2-x_1^2}}\right] dx_1 \,. \tag{128}$$

The integral I_1 is

$$I_1 = \tau b\left[x_1\log\left(\frac{\tau\sqrt{\beta_0^2-b^2} - \sqrt{\tau^2\beta_0^2-x^2}}{\sqrt{\tau^2\beta_0^2-x_1^2} + \tau\sqrt{\beta^2-x^2}}\right)\right.$$

$$+ \frac{\tau b}{2}\log\left(\frac{\tau^2\beta_0^2 + \tau bx_1 - \tau\sqrt{(\beta_0^2-b^2)(\tau^2\beta^2-x^2)}}{\tau^2\beta_0^2 - \tau bx_1 - \tau\sqrt{(\beta_0^2-b^2)(\tau^2\beta_0^2-x_1^2)}}\right)$$

$$- \frac{\tau b}{2} \log \left(\frac{\tau^2\beta_0^2 + \tau b x_1 + \tau\sqrt{(\beta_0^2-b^2)(\tau^2\beta_0^2-x_2^2)}}{\tau^2\beta_0^2 - \tau b x_1 + \tau\sqrt{(\beta_0^2-b^2)(\tau^2\beta_0^2-x_1^2)}} \right)$$

$$+ 2\tau\sqrt{\beta_0^2-b^2} \cos^{-1}\left(\frac{x_1}{\tau\beta_0}\right) \Bigg]_{\tau b}^{\tau\beta_0} \tag{129}$$

which reduces to the result

$$I_1 = \tau^2 b^2 \left\{ 2\log\left(\frac{\beta_0}{b}\right) - \frac{2\sqrt{\beta_0^2-b^2}}{b} \cos^{-1}\left(\frac{b}{\beta_0}\right) \right\} . \tag{130}$$

Considering next I_2,

$$I_2 = \frac{1}{2} \left[(x_1^2-\tau^2 b^2) \log \left(\frac{x_1\sqrt{\beta_0^2-b^2} + b\sqrt{\tau^2\beta_0^2-x^2}}{x_1\sqrt{\beta_0^2-b^2} - b\sqrt{\tau^2\beta_0^2-x_1}} \right) \right.$$

$$\left. -2\tau^2 b\sqrt{\beta_0^2-b^2} \cos^{-1}\left(\frac{x_1}{\tau\beta_0}\right) \right]_{b\tau}^{\beta_0\tau} \tag{131}$$

or

$$I_2 = \tau^2 b\sqrt{\beta_0^2-b^2} \cos^{-1}\left(\frac{b}{\beta_0}\right) . \tag{132}$$

Therefore, the derivative with respect to τ of Eq. (126) is:

$$\frac{\partial}{\partial\tau} \int_{b\tau}^{\beta_0\tau} u_2(x_1,\tau)dx = \frac{TA\tau b^2}{\rho c_1^2(\beta_0^2-b^2)^{3/2} b} \left[\frac{\sqrt{\beta_0^2-b^2}}{b} \cos^{-1}\left(\frac{b}{\beta_0}\right) \right.$$

$$\left. - 2 \log\left(\frac{\beta_0}{b}\right) \right] . \tag{133}$$

From Equation (122), the expression for $u_2(b\tau,\tau)$ is obtained to be

$$u_2(b\tau,\tau) = \frac{(b\tau)TA}{\rho c_1^2(\beta_0^2-b^2)^{3/2}b} \log(\frac{\beta_0}{b}) \tag{134}$$

and, from Equations (125), (133), and (134), it follows that G_I is

$$G_I = \frac{2YTA(b\tau)}{\rho c_1^2(\beta_0^2-b^2)^{32}b} \left[\frac{\sqrt{\beta_0^2-b^2}}{b} \cos^{-1}(\frac{b}{\beta_0}) - \log(\frac{\beta_0}{b}) \right]. \tag{135}$$

The energy release rate normalized with respect to the corresponding static elastic value is plotted in Figure 26 and may be compared to the elastic result for a crack of the same velocity and length.

A quantity mentioned previously as being of descriptive importance is the crack opening displacement, δ_T, at the point $|x_1|=vt$ where the plastic zone begins. This quantity is twice the displacement $u_y(b\tau,b)$, given by Equation (134), or

$$\delta_T = \frac{2cTA}{\rho c_1^2(\beta_0^2-b^2)^{3/2}b} \log(\beta_0/b) . \tag{136}$$

Since $\beta_0/b = a/c$, it is easily seen that Equation (136) is the same as Equation (100), the crack opening diplacement for the fixed length case. It should be noted, however, that for a fixed applied stress P, the behavior of δ_T with respect to crack velocity is not the same. This is due to the fact that in the steady state case, for which Equation (100) applies, the ratio a/c is dependent only on P/Y and is independent of crack velocity, while a change of crack velocity in

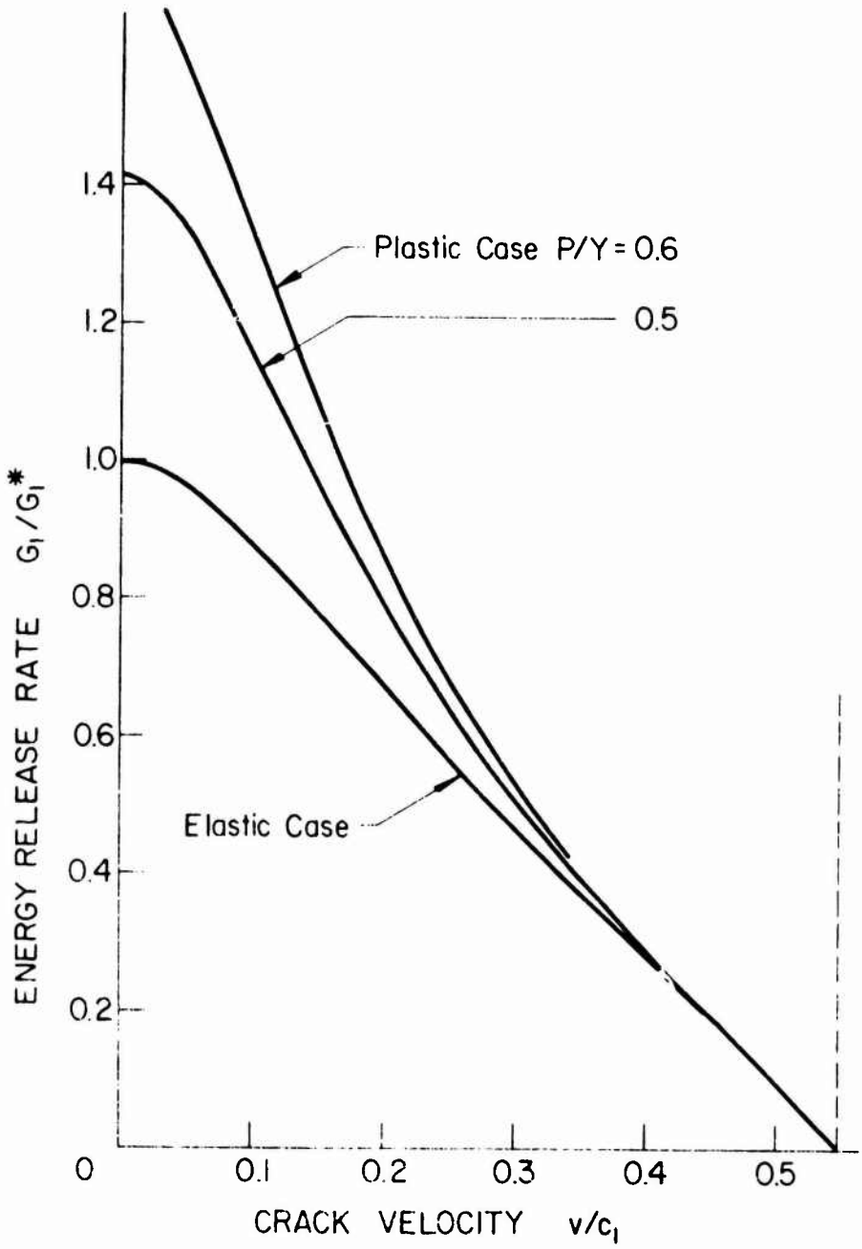

Figure 26. Normalized Energy Release Rate for Uniformly Expanding Crack Model.

Equation (136) when P/Y is fixed requires a change in β_0/b through the finiteness condition.

The relation $G_I = \delta_T Y$ has been used in Section IV for the static case. Multiplication of Eq. (136) by the yield stress Y and comparison with Eq. (135) reveals that this relationship does not apply here. The basic difference is that expanding crack model accounts for energy dissipation not only through the translation of the plastic region with the crack tip but also through enlargement of this plastic region. Therefore, one would expect that G_I, as given by Equation (135), would be higher than $\delta_T Y$. This is shown graphically in Figure 27 where the relative difference between G_I and $\delta_T Y$ is plotted as a function of normalized crack velocity b and in Figure 28 where the same difference is plotted as a function of P/Y.

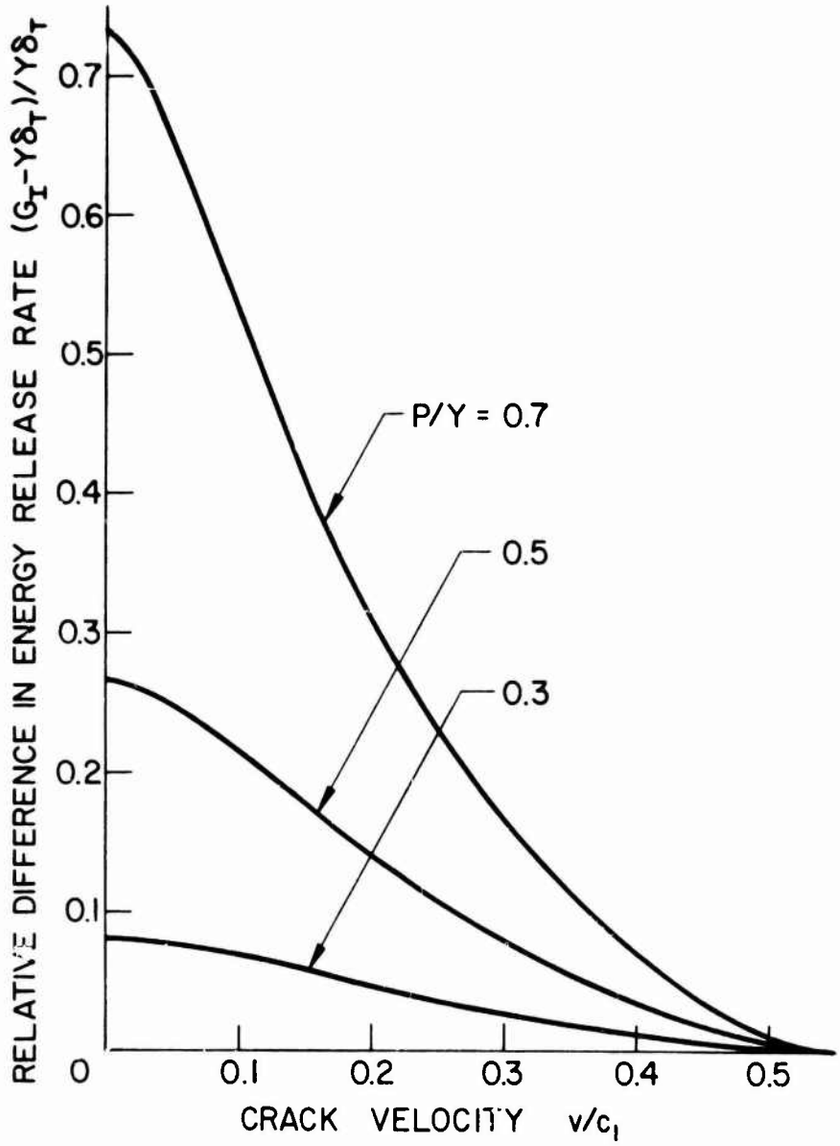

Figure 27. Relative Difference in Energy Release Rate for Expanding Crack Model Due to Difference in Method of Calculation Plotted as a Function of Crack Velocity.

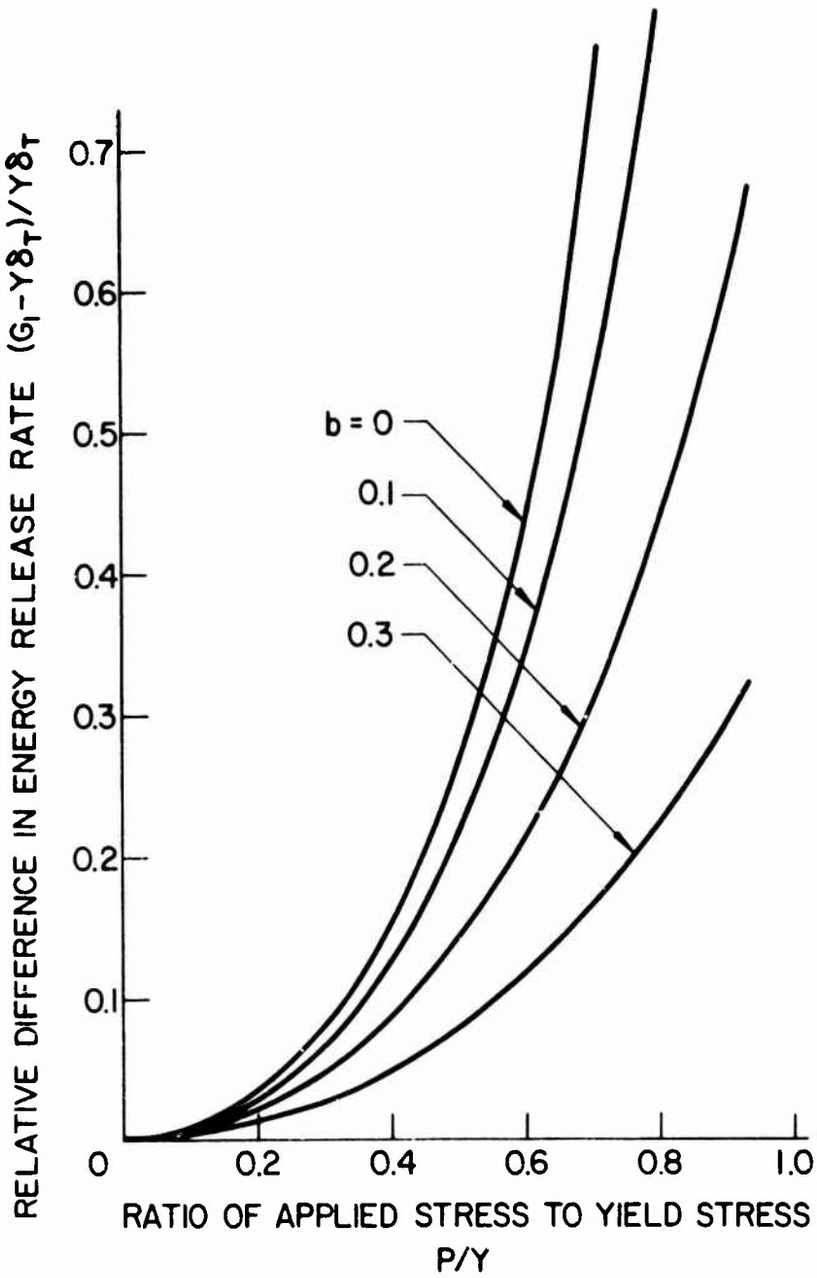

Figure 28. Relative Difference in Energy Release Rate for Expanding Crack Model Due to Method of Calculation Plotted as a Function of P/Y.

SECTION VI

RESULTS

General results have been presented in Section II that allow the calculation of the rate at which energy is released by a uniformly moving crack. Of particular interest is the fact that a path independent integral may be used for this calculation not only for the steady state cases of crack propagation but for the non-steady state case of the uniformly expanding crack, as modeled by Broberg.

The rate at which energy is dissipated due to plasticity was calculated, for the dynamic case, in a manner analagous to the analysis of Goodier and Field [28] for the static case. Although a specific result was presented only for perfect plasticity, work hardening can be incorporated through Equation (17).

In order to gain further insight into the transient response of the cracked plate, it is useful to review the wave patterns. When a transient load is applied to the crack surface, the result, aside from wave propagation from the loaded surface, is that the crack tips form the center of two outgoing cylindrical waves. For the period of time, t_s, before these waves begin to interact the short time behavior of the solution is described by the equations

$$\sigma_{ij} = \frac{k^{(s)}}{\sqrt{2r}} f_{ij}(\theta) \qquad 0<t\leq t_s$$

where r is the distance from the crack tip, and

$$k_{\ell}^{(s)} \approx \sqrt{t} \ .$$

The function $f_{ij}(\theta)$ is the same as in the static case. Since the disturbance at one crack tip is not yet affected by the presence of the other crack tip, this is the range for which the solution to the problem of sudden loading on a semi-infinite crack is valid. For normal loading the stress-intensity factor may be obtained from the solution of Baker [17] which is,

$$k_1^{(s)} = \sigma_1 \sqrt{a} \quad .785\sqrt{c_2 t/a)}$$

for the case of steel.

This result is plotted in Figure 9 and shows good agreement with the numerical solution obtained here.

The stress wave pattern loses its geometrical simplicity after the two cylindrical waves begin to interact although, very close to the crack tip, the angular distribution and square root singularity remain the same. It is during this period of maximum disorder that the stress-intensity factor takes on a maximum value. The pattern described here is shown in Figure 7 for various times after the initial loading. The outer wave front surrounding the crack is not to scale and is obtained by allowing a sufficient time to elapse such that $c_2 t >> 2a$. At this time enough energy has been transmitted away from the crack that

the dynamic-stress intensity factor is very close to the static value.

These results presented here are in agreement with those of Soltesz and Sommer[34] who experimentally determined the time-dependent stress-intensity factor due to normal loading of a crack in a finite plate of Araldit B. Measurements of the crack opening displacement, which is directly related to the stress-intensity factor, showed that k_1 reached a maximum at approximately 10^{-5} seconds, the same order of magnitude as obtained here. The oscillations that were observed in crack-opening displacement were explained as due to a combination of wave reflection at the edges of the finite plate and oscillation in the k_1 value due to the initially applied load, i.e., the result demonstrated in this work.

The results of Section IV for the steady-state cases may present some difficulty when an attempt is made to interpret them physically. This may be seen in the elastic case by examination of Figure 20 which applies for both the semi-infinite and constant length crack. If the assumption is made that the crack will run at a speed that causes G_I to be equal to a critical value G_{Ic}, then, for a given velocity, an increase in G_I^*, the corresponding static value of G_I, would have the effect of lowering the crack velocity in order to maintain the same critical value of G_I.

In the case of the semi-infinite crack, it can be argued that the result of an increase in the applied load P would be to increase the distance c from the crack tip, thus possibly maintaining the same value of G_I^*. The results for both the elastic and plastic case should have some use in considering the physical problem of a wedge load applied to the crack surface.

The character of the elastic stress-field ahead of a moving crack tip is the same for all constant velocity models of the same mode as stated in Appendix I. Thus, since the Yoffe model was the first dynamic crack model, the results, in this respect, were a valuable contribution. However, it is important to note that the model of a crack which opens at one end and closes at the other is physically unrealizable, and one should expect paradoxes in the result of any analysis. The fact that the results indicate an increase in the elastic energy release rate with velocity for a given load and crack length is such a paradox since, in effect, it says that for a given load the larger the crack length the lower the corresponding crack speed. Further, note in the elastic case that the energy release rate for the entire system is zero (no energy is transferred over a boundary surrounding and moving with the entire crack) while the energy release rate for one crack tip approaches infinity as the crack speed approaches the Rayleigh wave velocity. In the corresponding Dugdale model, the length of the plastic zone is independent of the crack velocity. This, in itself does

not agree with the analysis of the more realistic Broberg model. In addition, Equation (99) indicates that the displacements vary from zero to infinity along the crack surface when the crack speed approaches c_R. This violates the assumptions of infinitesimal strain theory and indicates the solution is invalid for large values of crack velocity.

It is the conclusion here that the Yoffe model should not be used to evaluate the quantitative effect of crack velocity on energy dissipation or plasticity and strain rate effects. Kanninen et al [29] used this model in dealing with strain hardening and strain rate effects. Their results are valid for low velocities since the value used for crack surface displacement is dependent on velocity through the function plotted in Figure 20. These authors, in fact, only used the Yoffe model as supporting evidence for the approximation of the dynamic case by the static values. Inspection of the corresponding curves for the Broberg model indicates that, while there is a range over which the quasi-static case may be used, it is not as large as anticipated by the results of Figure 20.

The Broberg model corrects many of the defects found in the Yoffe model. It more closely approximates the physical situation in that it takes into account the fact the crack is increasing in size. The elastic and plastic results for the strain energy release rate (Figure 26) follow a trend opposite to the Yoffe model, with G_I/G_I^*

approaching zero as $v \to c_R$. Therefore, although the results for both models have indicated the Rayleigh wave speed as an upper limit on crack velocity, the reasons are exactly opposite. Physically, the arguments for a limiting velocity based on either creation of surface energy (see sub-section 5.1) or plastic dissipation make more sense when used in conjunction with the Broberg model.

When the Dugdale criterion is incorporated into the Broberg model, the finiteness condition dictates that, for a fixed value of P/Y, larger normalized crack velocities b decrease the relative plastic zone size $(\beta_0 - b)/\beta_0$ (see Figure 23). In addition, at high velocities the plastic value of energy dissipation approaches the elastic value (Figure 26). These results are supported by experimental evidence which indicates that high velocity fracture is essentially a brittle process.

(The reverse of this page is blank)

APPENDIX I

ELASTIC PROBLEMS OF UNIFORM CRACK EXTENSION

In terms of polar coordinates r and θ with the origin at the crack tip as shown in Figure 1, Sih [3] has shown that, for a class of dynamic crack propagation problems in which the crack tip moves at a constant velocity v, asymptotic expansions of the dynamic stresses and displacements as $r \to 0$ can be found without specifying crack geometry and loading conditions.

For the opening mode of crack extension, where the loads are placed symmetrically with respect to the crack line, as in the Yoffé and Broberg models, the singular portion of the dynamic stress field near the crack tip is

$$\sigma_{11} = \frac{k_1}{\sqrt{2r}} F_1(s_1,s_2)[(1+s_2^2)(2s_1^2+1-s_2^2)f(s_1)-4s_1s_2f(s_2)] \tag{I-1}$$

$$\sigma_{22} = \frac{k_1}{\sqrt{2r}} F_1(s_1,s_2)[4s_1s_2f(s_2) - (1+s_2^2)^2f(s_1^2)] \tag{I-2}$$

$$\sigma_{12} = \frac{k_1}{\sqrt{2r}} 2s_1(1+s_2^2)F_1(s_1,s_2)[g(s_1)-g(s_2)] \ . \tag{I-3}$$

The corresponding displacement expressions are

$$\mu u_1 = k_1\sqrt{2r}\, F_1(s_1,s_2)[(1+s_2^2)(\cos^2\theta + s_1^2\sin^2\theta)f(s_1)$$

$$+ 2s_1s_2(\cos^2\theta + s_2^2\sin^2\theta)f(s_2)] \tag{I-4}$$

Preceding page blank

$$\mu u_2 = k_1\sqrt{2r}\, F_1(s_1,s_2)[s_1(1+s_2^2)(\cos^2\theta + s_1^2\sin^2\theta)g(s_1)$$

$$- 2s_1(\cos^2\theta + s_2^2\sin^2\theta)g(s_2)] \qquad \text{(I-5)}$$

where k_1 is the opening mode stress-intensity factor for the corresponding static case. The functions s_j $(j=1,2)$ are

$$s_j = [1 - (v/c_j)^2]^{\frac{1}{2}} \qquad j = 1,2 \qquad \text{(I-6)}$$

in which c_1 and c_2 are, respectively, the dilatational and shear wave velocities in an infinite elastic continuum. In terms of the shear modulus μ, Poisson's ratio ν, and the mass density ρ, c_1 and c_2 are

$$c_1 = \begin{cases} [2\mu(1-\nu)/\rho(1-2\nu)]^{\frac{1}{2}} & \text{, plane strain} \\ [2\mu/\rho(1-\nu)]^{\frac{1}{2}} & \text{, plane stress} \end{cases} \qquad \text{(I-7)}$$

$$c_2 = (\mu/\rho)^{\frac{1}{2}} . \qquad \text{(I-8)}$$

The quantities $f(s_j)$ and $g(s_j)$ describe the angular distribution of the stresses and displacements and are obtainable from:

$$\begin{aligned} f^2(s_j) + g^2(s_j) &= \sec\theta(1+s_j^2\tan^2\theta)^{-\frac{1}{2}} \\ f^2(s_j) - g^2(s_j) &= \sec\theta(1+s_j^2\tan^2\theta)^{-1} \end{aligned} \quad (j=1,2) \qquad \text{(I-9)}$$

The function $F_1(s_1 s_2)$ depends on the particular problem under consideration. For the crack of fixed length propagating at a uniform velocity, $F_1(s_1,s_2)$ is

$$F_1(s_1,s_2) = [4s_1 s_2 - (1+s_2^2)^2]^{-1} . \qquad \text{(I-10)}$$

For Broberg's solution,

$$F_1(s_1,s_2) = s_1\Big\{[(1+s_2^2)^2 - 4s_1^2 s_2^2]K(s_1) - 4s_1^2(1-s_2^2)K(s_2)$$
$$- [4s_1^2 + (1+s_2^2)^2]E(s_1)+8s_1^2 E(s_2)\Big\}^{-1}. \qquad \text{(I-11)}$$

The expression for k_1 is seemingly the same for both models, that is

$$k_1 = p\sqrt{c}$$

where c is one-half the crack length. However, for the Yoffé model c is constant whereas for the Borberg model c is a function of t. Thus, in calculating energy release rate, one should be aware of the restrictions in sub-section 2.3.

For a semi-infinite crack with the load and geometric configuration of Figure 12, $F_1(s_1,s_2)$ is also given by Equation (I-10) and the stress intensity factor k_1 is equal to $[(Q/\pi)\sqrt{(2/c)}]$.

APPENDIX II

NUMERICAL PROCEDURE

The dual integral equations formulated in Section III were reduced to a Fredholm integral equation that must be solved numerically. This integral equation is in the form

$$\Lambda^*(\xi,\kappa)-\int_0^1 \Lambda^*(\xi,\kappa)K(\xi,\kappa)d\eta = h(\xi) \qquad \text{(II-1)}$$

where $h(\xi)$ and $K(\xi,\eta)$ are known functions.

The method of solution that was chosen was to approximate the integral in Equation (II-1) by a finite sum and solve the following set of simultaneous linear equations for the unknowns $\Lambda(\xi_i,\kappa)$.

$$\Lambda^*(\xi_i,\kappa)-\sum_{j=1}^{N} a_j K(\xi_i,\eta_j)\Lambda(\eta_j,\kappa) = h(\xi_i) \qquad \text{(II-2)}$$

$$i = 1,\cdots, N .$$

The constants, a_j, are chosen in accordance with Simpson's rule and

$$\xi_i = \frac{(i-1)}{(N-1)} \quad , \quad \eta_j = \frac{(j-1)}{(N-1)} . \qquad \text{(II-3)}$$

The function Λ^* is thus approximated for each choice of the parameter, κ , which is related to the Laplace transform variable p by the equation,

$$\kappa = \frac{c_2}{ap} . \qquad \text{(II-4)}$$

By this means, for a given value of ξ, the function $\Lambda^*(\xi,\kappa)$ can be represented numerically in the Laplace transformed domain. The curve showing $\Lambda^*(1,\kappa)$ as a function of κ is shown in Figure 8.

In order to complete the solution for the near-field stress components, the function M(t) defined by Equation (53) must be evaluated. Noting that

$$L\left\{\int_0^t m(t)dt\right\} = \frac{1}{p} L\left\{m(t)\right\} , \qquad \text{(II-5)}$$

it follows from Equations (53) and (51) that

$$M(t) = L^{-1} [f^*(p)\Lambda^*(1,\kappa)]. \qquad \text{(II-6)}$$

For the particular example treated numerically, f(t) is the Heaviside step function and therefore $f^*(p)$ is $1/p$. The solution is then completed by evaluating numerically the inverse Laplace transform of the function $\Lambda^*(1,c_2/pa)/p$. The Laplace transform pair in question may now be written

$$\frac{\Lambda^*(1,c_2/pa)}{p} = \int_0^\infty M(t)\exp(-pt)dt \qquad \text{(II-7)}$$

$$M(t) = \frac{1}{2\pi i}\int_{Br} \frac{\Lambda^*(1,c_2 p/a)}{p} \exp(pt)dp . \qquad \text{(II-8)}$$

Make the following definition

$$s = \frac{pa}{c_2} = \frac{1}{\kappa} \qquad \text{(II-9)}$$

$$T = \frac{c_2 t}{a} \tag{II-10}$$

$$\Lambda_1^*(1,s) = \Lambda^*(1,1/s) \tag{II-11}$$

$$M_1(T) = M(t) = M(aT/c_2) \ . \tag{II-12}$$

Then, in terms of the variables s and T, the Laplace transform pair is

$$\frac{\Lambda_1^*(1,s)}{s} = \int_0^\infty M_1(T)\exp(-sT)dT \tag{II-13}$$

$$M_1(T) = \frac{1}{2\pi i}\int_{Br} \frac{\Lambda^*(1,s)}{s} \exp(sT)ds \ . \tag{II-14}$$

Having available the solution of Equation (II-1), $\Lambda_1^*(1,s)/s$ is known for discrete values of s. There are a number of methods available that allow calculation of a function from knowledge of a finite number of values of its Laplace transform. The one used here is due to Papoulis[35], as enlarged upon by Miller and Guy [36]. In this case, $\Lambda_1(1,s)/s$ is evaluated at points given by

$$s = (1+n)\delta \quad , \quad n = 0,1,2,\cdots, \tag{II-15}$$

where δ is a real positive number. In order to change the infinite range of integration in Equation (II-13) to a finite one, the following definitions are made:

$$x = 2\exp(-\delta T) - 1 \tag{II-16}$$

$$\psi(x) = M_1(T) = M_1(-\frac{1}{\delta}\,\ell n[(x+1)/2]). \tag{II-17}$$

Equation (II-13) is then changed to

$$\frac{\Lambda_1^*(1,[1+n]\delta)}{(1+n)} = \frac{1}{2^{n+1}}\int_{-1}^{1}(1+x)^n\psi(x)dx\ . \tag{II-18}$$

The function $\psi(x)$ is expanded in a series of Legendre polynomials orthogonal on the interval (-1,1) as follows

$$\psi(x) = \sum_{k=0}^{\infty} C_k P_k(x) \tag{II-19}$$

where

$$P_n(x) = \frac{(-1)^n}{2^n n!}\frac{d^n}{dx^n}[(1-x)^n(1+x)^n] \tag{II-20}$$

and,

$$\int_{-1}^{+1} P_n(x)P_m(x)dx = \begin{cases} 0 & n\neq m \\ \dfrac{1}{n+\frac{1}{2}} & n=m \end{cases}\ . \tag{II-21}$$

Note that

$$(1+x)^n = \sum_{k=0}^{n} a_k P_k(x) \tag{II-22}$$

where

$$a_k = 2^n(2k+1)\,\frac{n(n-1)\cdots[n-(k-1)]}{(n+1)(n+2)\cdots(n+k+1)}\ . \qquad \text{(II-23)}$$

Then, making use of Equations (II-21) through (II-23), substitution of Equation (II-19) into Equation (II-18) yields the following set of equations that may be solved for C_k:

$$\frac{\Lambda_1^*(1,[1+n]\delta)}{(1+n)} = \sum_{k=0}^{n} \frac{n(n-1)\cdots[n-(k-1)]}{(n+1)(n+2)\cdots(n+k+1)}\,C_k \qquad \text{(II-24)}$$

$$n=1,2,\cdots,$$

Note that, for n=0,

$$\Lambda_1^*(1,\delta) = C_0\ . \qquad \text{(II-25)}$$

If N coefficients are calculated, a partial sum is obtained from Equation (II-19), and by Equations (II-16) and (II-17) an approximation of $M_1(T)$ is given as

$$M_1(T) = \sum_{k=0}^{N-1} C_k P_k[2\exp(-\delta T)-1]\ . \qquad \text{(II-26)}$$

The parameter δ is chosen so that M(T) is best described for a particular range of T.

REFERENCES

(1) Sih, G. C., and Liebowitz, H., "Mathematical Theories of Brittle Fracture", Vol. 2, Mathematical Fundamentals of Fracture edited by H. Liebowitz, pp. 67-190, Academic Press, New York, 1968.

(2) Irwin, G. R., "Fracture Mechanics", Structural Mechanics, pp. 560-574, Pergamon Press, London, England, 1960.

(3) Sih, G. C., "Dynamic Aspects of Crack Propagation", in Inelastic Behavior of Solids, edited by M. F. Kanninen, W. F. Adler, A. R. Rosenfield, and R. I. Jaffe, pp. 607-639, McGraw-Hill, New York, 1970.

(4) Taylor, G. I., "The Formation and Enlargement of a Circular Hole in a Thin Plastic Sheet", Quarterly Journal of Mechanics and Applied Mathematics, Vol. 1, p. 103, 1948.

(5) Chou, P. C., "Perforation of Plates by High-Speed Projectiles", Developments in Mechanics, Vol. 1, Proceedings of the Seventh Midwestern Mechanics Conference, Edited by J. E. Lay and L. E. Malvern, Plenum Press, New York, 1961.

(6) Zaid, M. and Paul, B., "Mechanics of High Speed Projectile Perforation", Journal of the Franklin Institute, Vol. 264, p. 117, 1957.

(7) Thomson, W. T., "An Approximate Theory of Armor Penetration", Journal of Applied Physics, Vol. 26, p. 80, 1955.

(8) Cagniard, L., Reflection and Refraction of Progressive Seismic Waves, McGraw-Hill, 1962.

(9) Heyda, J. F., Woodall, S. R., Wolfgang, S. R., and Wilson, L. L., "A Combined Theoretical and Experimental Investigation of Armor Penetration Mechanics", Technical Report AFATL-TR-70-78, 1970.

(10) Atkinson, C., and Eshelby, J. D., "The Flow of Energy into the Tip of a Moving Crack", International Journal of Fracture Mechanics, Vol. 4, 1968.

(11) Broberg, K., "The Propagation of a Brittle Crack", Arkiv for Fysik, Vol. 18, p. 159, 1960.

(12) Rice, J. R., "Mathematical Analysis in the Mechanics of Fracture", in Fracture Vol. 2, edited by H. Liebowitz, Academic Press Inc., 1968.

(13) Dugdale, D. S., "Yielding of Steel Sheets Containing Slits", Journal of the Mechanics and Physics of Solids, Vol. 8, pp. 100-104, 1960.

(14) Atkinson, C., "A Simple Model of Relaxed Expanding Crack", Arkiv for Fysik, Vol. 35, pp. 469-476, 1968.

(15) Kostrov, B. V., "Unsteady Propagation of Longitudinal Shear Cracks", Prikladnaia Matematika I Mekanika (Journal of Applied Mathematics and Mechanics). Vol. 30, p. 1042, 1966.

(16) Maue, A. W., "Die Entspannungswelle bei plötzlichem Einschnitt eines gespannten elastichen Körpers", Zeitschrift fur Angewandte Mathematik und Mechanik, Vol. 34, pp. 1-12, 1954.

(17) Baker, B. R., "Dynamic Stresses Created By a Moving Crack", Journal of Applied Mechanics, Vol. 24. pp. 449-454, 1962.

(18) Sneddon, I. N., Fourier Transforms, McGraw-Hill, 1951.

(19) Doetsch, G., Guide to the Applications of Laplace Transforms, D. Van Nostrand, 1961.

(20) Sih, G. C., and Loeber, J. F., "Wave Propagation in an Elastic Solid with a Line of Discontinuity or Finite Crack", Quarterly of Applied Mathematics, Vol. 27, p. 193, 1969.

(21) Watson, G. N., A Treatise on the Theory of Bessel Functions, 2nd. ed., The MacMillan Co., New York, 1948.

(22) Whittaker, E. T., and Watson, G. N., A Course of Modern Analysis, 4th. Ed., Cambridge University Press 1927.

(23) DeHoop, A. T., "A Modification of Cagniard's Method for Solving Seismic Pulse Problems", Appl. Sci. Research, Sec. B. Vol. 8, pp. 349-356, 1960.

(24) Muskhelishvili, N. I., Singular Integral Equations, P. Noordhoff, N. V., 1953.

(25) Yoffé, E. H., "The Moving Griffith Crack", Philosophical Magazine, Series 7, Vol. 42, 1951.

(26) Craggs, J. W., "On the Propagation of a Crack in an Elastic Brittle Material," Journal of the Mechanics and Physics of Solids, Vol. 8, p. 66, 1960.

(27) Craggs, J. W., "Fracture Criteria for Use in Continuum Mechanics", in Fracture of Solids, Edited by Drucker and Gilman, pp. 51-63, Interscience, 1963.

(28) Goodier, J. N., and Field, F. A., "Plastic Energy Dissipation in Crack Propagation", in Fracture of Solids, edited by Drucker and Gil n, pp. 103-115, Interscience, 1963.

(29) Kanninen, M. F., Mukherjee,A. K., Rosenfield, A. R., and Hahn, G. T., "The Speed of Ductile Crack Propagation and the Dynamics of Flow in Metals", in Mechanical Behavior of Materials under Dynamic Loads, edited by U. Lindholm, pp. 96-133, Springer-Verlag, 1968.

(30) Muskhelishvili, N. I., Some Basic Problems of the Mathematical Theory of Elasticity, P. Noordhoff Ltd., 1963.

(31) Radok, J. R. M., "On Solutions of Problems of Dynamic Plane Elasticity", Quarterly of Applied Mathematics, Vol. 14, p. 289, 1956.

(32) Sih, G. C., "Some Elastodynamic Problems of Cracks", International Journal of Fracture Mechanics, Vol. 4, pp. 51-68, 1968.

(33) Byrd, P. F., and Friedman, M. D., Handbook of Elliptic Integrals for Engineers and Physicists, Springer-Verlag, 1954.

(34) Soltesz, U., and Sommer, E., "Crack-Opening-Displacement Measurement of a Dynamically Loaded Crack", Journal of Engineering Fracture Mechanics (in Press).

(35) Papoulis, A., "A New Method of Inversion of the Laplace Transform", Quarterly of Applied Mathematics, Vol. 14, p. 405, 1957.

(36) Miller, M. K., and Guy, W. T., "Numerical Inversion of the Laplace Transform by Use of Jacobi Polynomials", SIAM Journal of Numerical Analsis, Vol. 3, p. 624, 1966.

(The reverse of this page is blank)

Distribution List.
Not Filmed

Pg. 107

Unclassified

Security Classification

DOCUMENT CONTROL DATA - R & D

Security classification of title, body of abstract and indexing annotation must be entered when the overall report is classified)

1. ORIGINATING ACTIVITY (Corporate author) Institute of Fracture and Solid Mechanics Lehigh University Bethlehem, Pennsylvania 18015	2a. REPORT SECURITY CLASSIFICATION Unclassified 2b. GROUP

3. REPORT TITLE

MECHANICS OF IMPACT AND CRACK PROPAGATION
Phase I: Development of an Analytical Fracture Model of Projectile Penetration

4. DESCRIPTIVE NOTES (*Type of report and inclusive dates*)

Final Report - July 1970 to June 1971

5. AUTHOR(S) (*First name, middle initial, last name*)

G. C. Sih
G. T. Embley

6. REPORT DATE August 1971	7a. TOTAL NO. OF PAGES 113	7b. NO. OF REFS 36
8a. CONTRACT OR GRANT NO. F08635-70-C-0120	9a. ORIGINATOR'S REPORT NUMBER(S)	
b. PROJECT NO. 2549 c. Task Number 03 d. Work Unit 08	9b. OTHER REPORT NO(S) (*Any other numbers that may be assigned this report*) AFATL-TR-71-95 T+E	

10. DISTRIBUTION STATEMENT

Distribution limited to U.S. Government agencies only; [redacted]; distribution limitation applied August 1971. Other requests for this document must be referred to the Air Force Armament Laboratory (DLRD), Eglin Air Force Base, Florida 32542.

11. SUPPLEMENTARY NOTES Available in DDC	12. SPONSORING MILITARY ACTIVITY Air Force Armament Laboratory Air Force Systems Command Eglin Air Force Base, Florida 32542.

13. ABSTRACT

This report is concerned with the application of fracture mechanics theory to the problem of projectile penetration and the situation where an excessive amount of energy is available to damage the target material in the form of fracture followed by crack propagation. The conditions under which this phenomenom takes place depend on several parameters, such as the speed and shape of the projectile and the geometry and material of the target. These conditions have been simulated in the laboratory. The present investigation deals only with the development of an analytical fracture model of the projectile penetration problem using the theory of continuum mechanics.

The amount of energy required to produce a crack of certain size in a pre-stretched plate within a very short period of time is estimated by solving a system of dual integral equations. Computer programs are being developed. In addition, the energy supplied to maintain a running crack at a certain speed is obtained with results illustrated by graphs. The effects of plasticity and rate sensitivity of the material are also discussed in this report.

DD FORM 1 NOV 65 1473

Unclassified

Security Classification

Unclassified
Security Classification

14 KEY WORDS	LINK A ROLE	LINK A WT	LINK B ROLE	LINK B WT	LINK C ROLE	LINK C WT
Projectile Penetration						
Crack Propagation						
Fracture Mechanics						
Energy Release Rate						
Plasticity						
Constant Velocity						
Target Material						

DD FORM 1 NOV 65 1473

Unclassified
Security Classification